



ELSEVIER

Contents lists available at ScienceDirect

Deep-Sea Research II

journal homepage: www.elsevier.com/locate/dsr2

Biogeochemical relationships between ultrafiltered dissolved organic matter and picoplankton activity in the Eastern Mediterranean Sea

Travis B. Meador^{a,b,g,*}, Alexandra Gogou^{a,b}, Georgina Spyres^{a,c}, Gerhard J. Herndl^{d,e}, Evangelia Krasakopoulou^a, Stella Psarra^f, Taichi Yokokawa^c, Daniele De Corte^{c,e}, Vassilis Zervakis^b, Daniel J. Repeta^g

^a Hellenic Centre for Marine Research, Institute of Oceanography, 46.7 km Athens-Sounion Av., 19013 Anavyssos, Greece

^b University of the Aegean, Department of Marine Sciences, 81100 Mytilene, Lesvos, Greece

^c Dept. of Biological Oceanography, Royal Netherlands Institute for Sea Research (NIOZ), PO Box 59, 1790AB Den Burg, The Netherlands

^d Univ. of Vienna, Ecology Center, Dept. of Marine Biology, Althanstr. 14, 1090 Vienna, Austria

^e Center for Ecological and Evolutionary Studies, University of Groningen, PO Box 14, 9750 AA Haren, The Netherlands

^f Hellenic Center for Marine Research, Institute of Oceanography, 71003 Heraklion, Crete, Greece

^g Department of Marine Chemistry and Geochemistry, Woods Hole Oceanographic Institution, Woods Hole, Massachusetts 02543, USA

ARTICLE INFO

Article history:

Received 20 April 2009

Accepted 10 December 2009

Available online 7 March 2010

Keywords:

DOM

biogeochemical cycles

Ultrafiltration

AOU

Microbial loop

ABSTRACT

We targeted the warm, subsurface waters of the Eastern Mediterranean Sea (EMS) to investigate processes that are linked to the chemical composition and cycling of dissolved organic carbon (DOC) in seawater. The apparent respiration of semi-labile DOC accounted for $27 \pm 18\%$ of oxygen consumption in EMS mesopelagic and bathypelagic waters; this value is higher than that observed in the bathypelagic open ocean, so the chemical signals that accompany remineralization of DOC may thus be more pronounced in this region. Ultrafiltered dissolved organic matter (UDOM) collected from four deep basins at depths ranging from 2 to 4350 m exhibited bulk chemical (¹H-NMR) and molecular level (amino acid and monosaccharide) abundances, composition, and spatial distribution that were similar to previous reports, except for a sample collected in the deep waters of the N. Aegean Sea that had been isolated for over a decade. The amino acid component of UDOM was tightly correlated with apparent oxygen utilization and prokaryotic activity, indicating its relationship with remineralization processes that occur over a large range of timescales. Principal component analyses of relative mole percentages of monomers revealed that oxygen consumption and prokaryotic activity were correlated with variability in amino acid distributions but not well correlated with monosaccharide distributions. Taken together, this study elucidates key relationships between the chemical composition of DOM and heterotrophic metabolism.

Published by Elsevier Ltd.

1. Introduction

1.1. Dissolved organic matter (DOM) cycling

Oceanic dissolved organic carbon (DOC) is one of the largest reservoirs of carbon on Earth, and its potential for exchange with other carbon reservoirs has brought it within the focus of global carbon-cycle research (Williams and Druffel, 1988; Toggweiler, 1989; Hedges, 1992; Hansell, 2002). The euphotic zone is the principal site of organic matter production in the open ocean.

* Corresponding author at: Department of Marine Chemistry and Geochemistry, Woods Hole Oceanographic Institution, Woods Hole, Massachusetts 02543, USA, Tel.: 508 289 3955; fax: 508 457 2075.

E-mail address: tmeador@whoi.edu (T.B. Meador).

¹ Present address: Department of Marine Chemistry and Geochemistry, Woods Hole Oceanographic Institution, Woods Hole, Massachusetts 02543, USA

The magnitude and composition of DOM produced during bloom events vary considerably and are controlled by a number of biological, chemical and physical parameters (Carlson, 2002). In the surface ocean, DOC stocks exceeding the deep refractory pool are composed of 'labile' and 'semi-labile' DOC (Hansell and Carlson, 1998a). Because labile DOC concentrations represent a very small fraction of bulk DOC (0–6%), the vertical gradient of the bulk DOC observed in stratified systems is mostly comprised of 'semi-labile' DOM (Carlson and Ducklow, 1995; Cherrier et al., 1996). The labile component of DOC arising from autotrophic production in the surface ocean is thought to support production of heterotrophic bacterioplankton (i.e. the microbial loop; Azam et al., 1983), and is either repackaged into bacterial organisms and passed to higher trophic levels or remineralized. Semi-labile DOC escapes rapid degradation by marine heterotrophs in surface ocean waters and is available for export to the ocean's interior by convective mixing (Copin-Montegut and Avril, 1993; Carlson

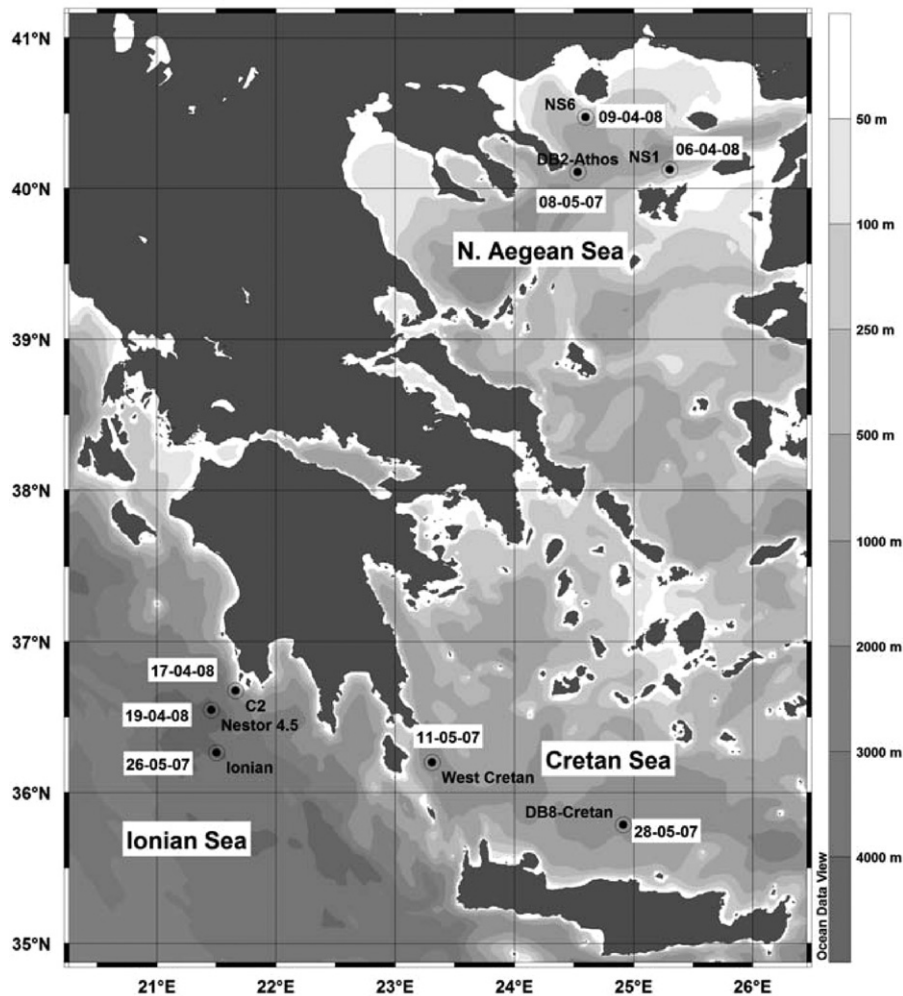


Fig. 1. UDOM sampling stations (circles) collected during POSEIDON, SESAME, and KM3NET cruises in May 2007 and April 2008. Sampling dates are provided adjacent to the location.

et al., 1994), advection along isopycnals surfaces (Hansell and Carlson, 2001), or sorption onto sinking particles (Keil and Kirchman, 1994; Druffel et al., 1996). This fraction can amount to 1.2 Gt C yr^{-1} , or 17% of global new production (Hansell and Carlson, 1998b) and provides a carbon source that fuels production by deep-sea free-living prokaryotes (Karner and Herndl, 1992; Smith et al., 1992; Nagata et al., 2000, 2010).

1.2. Oceanographic setting

The Mediterranean Sea has often been described as a small ocean as it encompasses all oceanic processes at much smaller time and space scales (Béthoux et al., 2002). Its thermohaline cell is forced by deep-water formation at the northern coasts of the Mediterranean during winter, and the formation of Levantine Intermediate waters in the northern part of the Eastern Mediterranean. In its eastern part, the Eastern Mediterranean Sea (EMS) is an ultra-oligotrophic environment characterized by extremely low dissolved nutrient concentrations, chlorophyll-*a* concentrations, and phytoplankton biomass in surface waters (Krom et al., 2003). The EMS is unique among the oligotrophic oceans because the ratio between dissolved nitrate and phosphate is higher than 20 in all sub-thermocline water masses (Krom et al., 1992; Béthoux et al., 2002). Its annual primary productivity is $60\text{--}80 \text{ g C m}^{-2} \text{ y}^{-1}$ (Ignatiadis, 1998; Psarra et al., 2000),

approximately half that determined in the oligotrophic Sargasso Sea (e.g., $157 \pm 7 \text{ g C m}^{-2} \text{ y}^{-1}$, Brix et al., 2006).

The area under investigation in this study extends throughout the Aegean Sea and into the Cretan and Ionian Seas (Fig. 1). Complex sea-bed topography together with Black Sea Waters (BSW) entering through the Dardanelles Straits and highly saline waters of Levantine origin determine the structure of the water column in the Aegean and, partly, the Ionian Seas. The surface layer of the north – northwest Aegean is covered by a light, thin layer of (BSW) of salinity as low as 30–35. The depths between 70 and 400 m in the North Aegean are waters with southeast Aegean / Levantine origin and are identified as the Levantine Intermediate Water (LIW; Lascaratos, 1993; Tzipperman and Speer, 1994), the most voluminous water mass of the Mediterranean (estimated at $2\text{--}3.5 \times 10^{13} \text{ m}^3$; Myers and Haines, 2000).

Below the LIW, the deep basins of the North Aegean are filled with locally formed North Aegean Deep Water (NAeDW). These waters form at infrequent intervals, as their high density hinders renewal and ventilation. The current NAeDW was formed during two major dense water formation events in the winters of 1992 and 1993 (Zervakis et al., 2000). Since then, the properties have evolved as a result of turbulent vertical mixing with the overlying LIW (Zervakis et al., 2003). During mild winters, LIW in the northeastern Aegean can be further subducted in an annual process that contributes to the formation Cretan Deep Water (CDW) (Zervakis et al., 2004; Gertman et al., 2006). The latter water mass thus contains higher dissolved

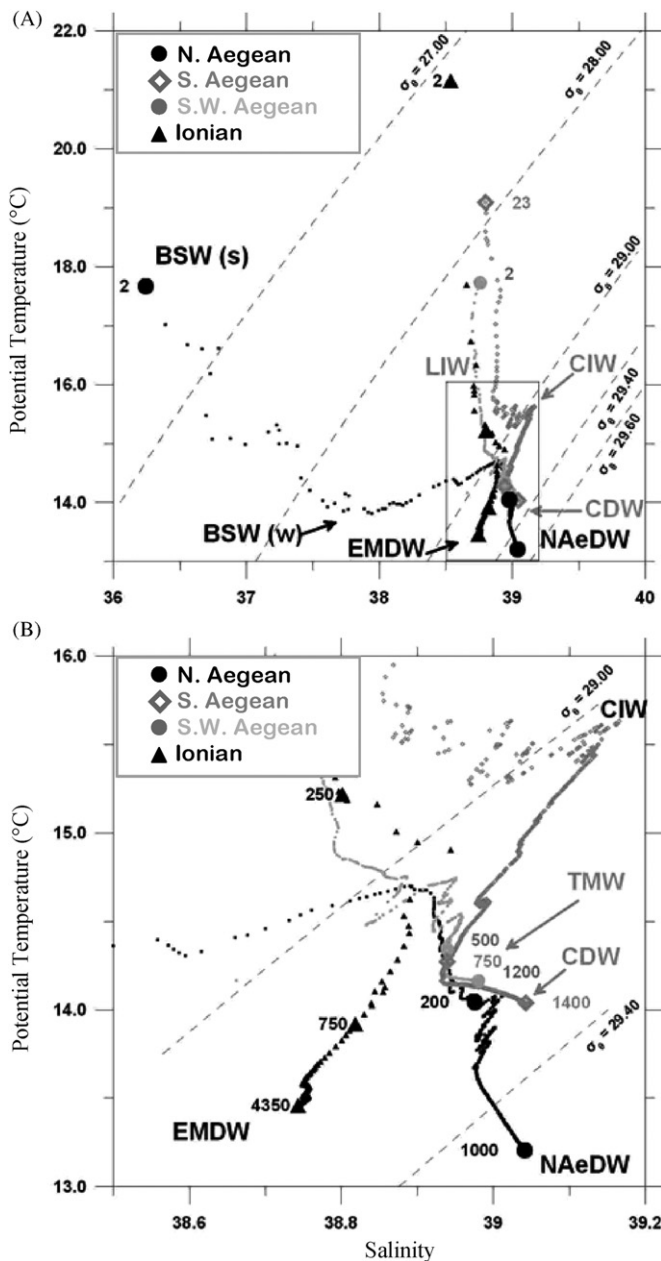


Fig. 2. Temperature-salinity diagrams for stations sampled in the N. Aegean (filled circles), S. Aegean (diamonds), S.W. Aegean (grey circles), and Ionian seas (filled triangles). Enlarged symbols represent stations and depths (m) where water was sampled for ultrafiltration. See Section 1.2 for water mass abbreviations.

oxygen than the deep layer of the North Aegean. Comparative analysis of T/S diagrams (see also Fig. 2b) suggests a significant contribution of North Aegean Sea water to CDW.

The layers between 400 and 900 m in the South Aegean (Cretan Sea) are characterized by a salinity minimum, signifying the Transitional Mediterranean Water mass (TMW), a mixture of LIW and Eastern Mediterranean Deep Waters (EMDW), the bottom waters of the Eastern Mediterranean found in the Ionian and Levantine Seas. TMW enters the Cretan Sea through the Cretan Straits, and its signature in the Cretan Sea is stronger when the exchange through the Straits intensifies. In this region above 400 m, a salinity maximum identifies the Cretan Intermediate Water, a locally formed water analogous to LIW, but with higher salinity. Lower salinities often found at the surface have been attributed to the inflow of Atlantic water through the Cretan

Straits (Theocharis et al., 1999) and more recently to BSW (Zervakis, Georgopoulos 2002).

The water column in the Ionian Sea is composed of a surface water mixture of Levantine, Cretan Sea, and Atlantic Waters, a LIW layer down to about 700 m, the TMW mass between 800 and 1000 m, and the EMDW masses, which comprises deep water of different origins formed during different generations of the Eastern Mediterranean Transient (Roether et al., 2007). The TMW mass, both in and outside the Cretan Sea, is probably the oldest of all types of water found in the region as it consists of a mixture of LIW with the oldest EMDW.

1.3. Objective

Previous reports have noted the inventory of total organic carbon (TOC) in the Mediterranean Sea (about 3 Pg C; Sempéré et al., 2000) and an average turnover time of “excess TOC” (i.e., semi-labile TOC) of 0.47 years in the N. Aegean and 0.28 years in the S. Aegean Seas (Sempéré et al., 2002). Additional details of the processes that control DOM reactivity in the EMS could be revealed by simultaneous measurements of DOM and microbial composition. In this study, we determined the total bulk chemical composition (inorganic nutrients, DOC), prokaryotic abundance and molecular-level chemical composition of UDOM in order to investigate the biological and chemical signatures that accompany respiration and the turnover of marine UDOM in this unique, oligotrophic marine environment. Emphasis is put on DOM production and degradation processes that occur in the mesopelagic (200 to 1000 m) and bathypelagic waters (> 1000 m) of the EMS, which exhibit higher temperatures (> 13 °C), higher oxygen consumption rates ($0.53 \mu\text{mol O}_2 \text{ kg}^{-1} \text{ y}^{-1}$; Roether and Well, 2001) and enhanced microbial activity relative to the bathypelagic Atlantic (Martín-Cuadrado et al., 2007). Our sample set includes depths to 4350 m, but we categorize samples as representative of either surface or subsurface waters (i.e., above or below the euphotic zone, respectively), paralleling the surface and mesopelagic realms of the open ocean.

We collected ultrafiltered DOM (UDOM; > 500 Da) from eight distinct water masses in the EMS. This approach is one of only a few methods that isolates DOM from the more abundant salts in seawater, thus permitting enhanced chemical characterization of the high molecular weight (HMW) component of DOM (e.g., Benner et al., 1992; McCarthy et al., 1996; Aluwihare et al., 1997, 2002; Meador et al., 2007). Correlations between apparent oxygen utilization (AOU) and TOC were used to estimate the proportion of carbon demand supported by TOC, and the molecular level composition of UDOM was determined to identify the chemical alterations that accompany the removal of the ‘semi-labile’ pool of DOC (also ‘exportable TOC’, Hansell, 2002; and ‘excess TOC’, Sempéré et al., 2002) that escapes degradation in surface waters. Also, direct comparisons are drawn between the bulk chemical (e.g., $^1\text{H-NMR}$) and molecular level composition (e.g., amino acid and monosaccharide distribution) of UDOM and local prokaryotic abundance and productivity. This analysis serves to further delineate the linkages between microbial metabolism and UDOM degradation processes in the ultra-oligotrophic and net heterotrophic Eastern Mediterranean basin.

2. Methods

2.1. Sampling

Samples were collected onboard the oceanographic vessel R/V AEGAE0, during the POSEIDON (May 2007), SESAME (April 2008)

and KM3Net (April 2008) cruises. A SBE-9 Plus Sea-Bird CTD profiler was used for data acquisition; this was equipped with pressure, temperature, conductivity, dissolved oxygen, fluorescence and light transmission sensors. The CTD salinity data were calibrated against water sample salinity measured using an AUTOSAL salinometer. The CTD profiler was mounted on a 24-Niskin-bottle rosette sampler, used to obtain sub-surface water samples. Surface water samples were collected using an air-pressure driven membrane pump and Teflon® tubing. Eight stations (Fig. 1) were selected in sub-basins in the north and south Aegean Sea and the southeastern Ionian Sea to represent various water masses of the E. Mediterranean. UDOM samples were collected at depths ranging from 2 to 4350 m at four stations during the POSEIDON cruise in May 2007 (station names: N. Aegean, S. Aegean, SW Aegean and Ionian; Table 1). At these stations, samples were also collected to determine depth profiles of inorganic nutrients (i.e., DIN, DIP), organic matter (i.e., TOC, UDOM chemical characterization) and biological parameters including prokaryotic abundance and activity, and community structure.

2.2. Inorganic Nutrients

Nutrient samples were collected in pre-cleaned polyethylene bottles and stored at -20°C until analysis in the laboratory. Dissolved inorganic nitrogen (DIN) was measured with a Bran+Luebbe II autoanalyzer following the method described by Strickland and Parsons (1972). Phosphate (DIP) was measured with a Perkin Elmer 20 Lambda UV/VIS Spectrometer according to the method of Murphy and Riley (1962).

2.3. Dissolved organic carbon (DOC)

For DOC determination, unfiltered samples from > 150 m were pipetted into combusted (450°C for 4 h) glass ampoules, immediately acidified with 3 to 4 drops of 45% H_3PO_4 and then flame sealed. Surface water samples collected above 150 m were filtered through rinsed $0.2\text{-}\mu\text{m}$ polycarbonate filters. Samples were stored at -20°C until analysis. DOC analysis was performed using the high temperature combustion method on a modified Shimadzu TOC-5000 A (Hansell, 1993; Spyres et al., 2000). The sample was automatically injected in quadruplicate onto a platinumized aluminum catalyst at a combustion temperature of 680°C . DOC concentrations in samples were determined relative to standards prepared using potassium hydrogen phthalate in Milli-Q water and consensus reference materials for DOC provided by the NSF-CRM program (<http://www.rsmas.miami.edu/groups/biogeochem/CRM.html>). The overall analytical precision was always $< 3\%$. For simplicity, we use the term DOC when referring specifically to the measurements of both the filtered (surface) and un-filtered samples (see Hansell 2002), and in reference to the more abstract global reservoir of carbon.

2.4. Dissolved oxygen

Samples for the determination of oxygen were first taken from the Niskin bottles with the recommended precautions to prevent any biological activity and gas exchange with the atmosphere, and titrated immediately afterward using a Dosimat Metrohm according to the Winkler method (Carpenter, 1965a, b). This method was consistent with other determinations of oxygen in seawater; the precision of the method was $\sim 2.2\ \mu\text{mol O}_2\ \text{L}^{-1}$ (Klein et al., 2003). The apparent oxygen utilization (AOU) was calculated according to the difference of the measured oxygen

Table 1
Bulk hydrographic and chemical measurements of seawater collected from ultrafiltration during the Poseidon, Sesame, and KM3Net research cruises. nd = no data; σ_t = sigma-teta density; AOU = apparent oxygen utilization; DOC = dissolved organic carbon.

Cruise	Sample	Date	Lat. ($^{\circ}\text{N}$)	Lon. ($^{\circ}\text{E}$)	Depth (m)	Salinity	Temp. ($^{\circ}\text{C}$)	σ_t (kg m^{-3})	AOU ($\mu\text{mol L}^{-1}$)	DOC ($\mu\text{mol L}^{-1}$)	Vol. (L) ultrafiltered	% DOC retained, ultrafiltered	% DOC retained, diafiltered ^a
POSEIDON	N. Aegean	8-May-07	40.109	24.531	2	36.245	17.669	26.309	-8.624	120	185	24	10 ± 1
					200	38.976	14.073	29.255	21.109	62	240	29	28
	S.W. Aegean	11-May-07	36.200	23.308	1000	39.041	13.353	29.485	59.296	53	150	39	9 ± 1
					2	38.759	17.729	28.224	-5.393	84	180	47	33
Ionian		26-May-07	36.265	21.502	500	38.939	14.420	29.161	26.256	54	220	54	40 ± 6
					1200	38.980	14.351	29.232	46.675	52	305	44	39 ± 3
					2	38.535	21.146	27.149	-4.628	77	300	43	18 ± 2
					250	38.801	15.255	28.858	19.323	65	170	61	37
S. Aegean		28-May-07	35.787	24.912	750	38.819	14.031	29.161	61.703	50	170	64	17
					1400	38.743	14.190	29.201	48.953	48	170	76	51 ± 3
					2	nd	nd	nd	-8.43	78	210	nd	25
					2	38.939	14.389	29.176	35.161	54	210	nd	20
SESAME	N. Aegean NS1	6-Apr-08	40.127	25.305	2	39.040	14.255	29.304	37.823	48	210	nd	22
					2	33.802	12.725	25.52	-4.993	120	400	nd	15 ± 2
KM3Net	K-C2	17-Apr-08	36.676	21.660	2	35.117	13.413	26.4	-1.284	95	100	nd	27 ± 2
					2	38.557	16.049	nd	nd	82	200	nd	19
	Nestor 4.5	19-Apr-08	36.548	21.459	2	38.575	16.286	nd	nd	91	150	nd	13

^a \pm error is based on the DOC concentration of ultrafiltered and diafiltered DOC retentates and is shown only for samples with error $\geq 1\%$

values to the oxygen saturation given by the Benson and Krause equation (UNESCO 1986).

2.5. Enumeration of picoplankton

Picoplankton abundance was determined in seawater collected from the Niskin bottles and fixed with 0.2- μm filtered formaldehyde (2% final concentration). Thereafter, the samples were frozen in liquid nitrogen for 10 min, then kept at -80°C until analysis. Picoplankton abundance was determined by flow cytometry within two months of collection. Samples were thawed to room temperature and 0.5-mL subsamples were stained with SYBR Green I in the dark for 10 min; subsequently, 1 μm fluorescent latex beads (Molecular Probes) (approximately 10^5 mL^{-1}) were added to the samples as internal standard. The picoplankton were enumerated on a FACScalibur flow cytometer (Becton Dickinson) by their signature in a plot of green fluorescence versus side scatter, and the abundance was calculated based on the ratio of stained cells to the internal standard. To convert cell abundance to picoplankton carbon biomass, a carbon content of 20 fg C cell^{-1} was used (Fukuda et al., 1998); this conversion likely overestimates picoplankton biomass but is used as a conservative estimate in terms of considering the possibility of contamination of DOC measurements by C directly associated with picoplankton biomass.

2.6. Prokaryotic activity

^3H -leucine incorporation rates were determined as a proxy for heterotrophic prokaryotic production (Kirchman, 2001). Subsamples (5–40 mL) from each depth were amended with 5 nmol L^{-1} ^3H -leucine (Amersham, specific activity: 160 Ci mmol^{-1}) and incubated at in situ temperature ($\pm 1^\circ\text{C}$) in the dark. Incubation time varied depending on depth: 1 h for upper waters ($< 100\text{ m}$) and 24 h for deep waters ($> 100\text{ m}$). After incubation, samples were filtered onto polycarbonate filters (pore size, 0.2 μm , Millipore) and rinsed twice with both 5% trichloroacetic acid and 80% ethanol. The samples were radio-assayed with a liquid scintillation counter (1211 Rackbeta, Wallac) using FilterCount scintillation cocktail (Packard). Duplicate samples and one trichloroacetic acid-killed control were prepared for each depth. The disintegrations per minute (DPM) of the killed control were subtracted from the mean DPM of the corresponding duplicate samples and the resulting count converted into leucine uptake rates.

2.7. Ultrafiltration

Water samples (150 to 300 L) collected during the POSEIDON May 2007 cruise were prefiltered through 0.2- μm cartridge filters (Gelman Criticap, USA). Ultrafiltered dissolved organic matter (UDOM) was obtained by concentrating these prefiltered samples using a custom-made Amicon SP-60 tangential-flow ultrafiltration system equipped with a Kock (Germany) spiral-wound polyamide 500 Dalton cut-off filter cartridge (operating pressure 3.0–5.5 bar, filter area 7.9 m^2 , filtrate flow rate 192 L h^{-1} at 3.0 bar) cleaned with 0.1 mol L^{-1} sodium hydroxide between samples. The samples were concentrated to about 6 L and stored frozen at -20°C for transport to the laboratory. Aliquots of ultrafiltered samples for amino acid analysis were collected in precombusted glass vials, then flame sealed and frozen until analysis. In the laboratory, most salts were removed from the concentrated samples by diafiltration with 10 volumes (i.e., 60 L) of MilliQ water, then lyophilized to a dry powder. UDOM samples that were concentrated and frozen after collection during the spring 2007 POSEIDON cruise exhibited a high-salt precipitate when thawed for

desalting. This precipitate was removed by filtering through GF/F (Whatman) before diafiltration of the dissolved sample; we are unsure of the carbon content of this precipitate.

Large volume seawater samples (150 to 200 L) collected during the SESAME (NS1 and NS6) and KM3Net (4.5 and C2) cruises were pumped exclusively from surface waters and prefiltered through 0.5- μm (Millipore Opticap XL4, USA) and 0.2- μm cartridge filters (Dornnick Hunter, UK), then ultrafiltered using a 500 Da (nominal molecular weight cutoff, MWCO) spiral wound cartridge (Separation Engineering Inc. GE2540F1072, operating pressure $< 3.0\text{ bar}$, filter area 1.9 m^2 , filtrate flow rate 30 L h^{-1}). Immediately after ultrafiltration, concentrated samples were diafiltered with $\sim 80\text{ L}$ of MilliQ water; volumes were reduced to $< 4\text{ L}$ and stored at -20°C . Frozen samples were lyophilized in the laboratory, or aliquots of concentrated UDOM solution were used for composition analyses.

2.7.1. Proton (^1H) nuclear magnetic resonance (NMR) spectroscopy

Approximately 20 to 200 mg of dried UDOM samples were dissolved in 0.75 mL of deuterated water (D_2O) and ^1H -NMR spectra were determined on a 400 MHz Bruker NMR arian INOVA NMR-lar weight cut off of easurements with typically > 2000 scans. The HDO peak was referenced to 4.76 ppm and was repressed in some cases. ^1H -NMR spectra were integrated with Mestre-C software according to chemical shift ranges defined as: aliphatic (C-CH-C, 0.5 to 1.8 ppm), alpha-substituted (O-C-CH-C, 1.8 to 3.2 ppm), and heteroatom substituted (O-CH-C or N-CH-C, 3.2 to 4.6 ppm). Resonances that appeared more downfield than 4.6 ppm (e.g., protons attached to unsaturated or aromatic carbons), were evident in some spectra, but were minimal and obscured by the peak arising from water; these were excluded from the analysis.

2.7.2. Monosaccharide analysis

The distributions of individual monosaccharides were determined for UDOM samples after diafiltration. Aliquots of UDOM samples representing 2.6 to 6.7 $\mu\text{mol C}$ were hydrolyzed in 0.5 mL 2 mol L^{-1} trifluoroacetic acid (TFA) with $40\text{ }\mu\text{g mL}^{-1}$ myo-inositol at 120°C for 2 h. Samples were then dried under a stream of N_2 gas and traces of acid were removed from the hydrolysate with subsequent resuspension and evaporation of isopropanol. Monosaccharides were reduced and acetylated to produce alditol acetates according to Aluwihare et al. (2002). Alditol acetates were separated by gas chromatography with a 30 m HP-5 fused silica column, with on-column injection at 270°C . After injection of 2 to 5 μL of sample, the oven temperature was held at 100°C for 1 min, then increased to 280°C at 3°C min^{-1} , and held at this temperature for the final 8 min. Alternatively, samples were injected with an injection port temperature that followed the oven gradient, holding at 50°C for 2 min, then ramping to 230°C at 5°C min^{-1} , then holding at 280°C for the final 8 min. Alditol acetates were identified by retention time and relative abundances were determined by the FID response of standards. Monosaccharides identified in this study included rhamnose (rham), fucose (fuc), arabinose (arab), xylose (xyl), mannose (man), galactose (gal), and glucose (glc). We were unable to quantify total yields of alditol acetates as the peak areas generated by monosaccharide standards were not reproducible; we attribute this complication to the on-column injection and to the HP-5 column. We recommend using a Supelco (SP2330) column with split injection. However, the relative peak areas of individual monosaccharides in standard and sample replicate injections were consistent ($\pm 0.6\%$), so we report monosaccharide mole percentages of UDOM samples.

Carbohydrate abundances were determined using the TPTZ method of Mykkestad et al. (1997), modified by Panagiotopoulos and Sempéré (2005), after hydrolysis of UDOM in 2 mol L⁻¹ TFA at 120 °C for 2 h. Aliquots of UDOM solutions used for this analysis ranged from 62 to 408 nmol C. Data are reported as dissolved combined neutral sugar concentration (DCNS) and as the percent of UDOC that is neutral sugar carbon (%NS-UDOC)

2.7.3. Amino acid analysis

Samples were collected directly from the ultrafiltration system, pipetted into combusted (450 °C for 4 h) 10-mL glass ampoules, flame sealed and stored frozen at -20 °C for transport to the laboratory for analysis. Samples were thawed and processed following the methodology of Fitznar et al. (1999) and Pérez et al. (2003). Hydrolysis was performed by adding HCl and ascorbic acid to 2 mL of sample and subsequently flushing with N₂. The pre-combusted glass ampoules were then sealed and incubated at 110 °C for 24 h. The hydrolyzed samples were dried and resuspended in a borate buffer (pH 8.5).

After hydrolysis, the concentrations of the individual amino acids were determined by high performance liquid chromatography (HPLC) of duplicate injections after pre-column derivatization with *o*-phthalaldehyde and *N*-isobutyryl-L-cysteine (Fitznar et al., 1999; Pérez et al., 2003). An integrated HPLC system was used consisting of a fluorescence detector (set at Ex: 330 nm; Em 445 nm) and autosampler for automatic derivatization. For separation of the individual amino acids, we used a C-12 reversed phased column and solvents and a multistep gradient system as described in Fitznar et al. (1999) as modified by Pérez et al. (2003). Amino acids were identified and quantified in relation to external standards. The *N*-isobutyryl-D-cysteine isomer was not used for derivitization as repeatable and clean chromatograms were generated using this method. Using these conditions, we measured glycine (gly), the D and L-enantiomers of aspartic acid and asparagine (asx, D-asx), glutamic acid and glutamine (glx, D-glx), serine (ser, D-ser), alanine (ala, D-ala), and tyrosine (tyr, D-tyr), as well as the L-enantiomers of threonine (thr), histidine (his), arginine (arg), valine (val), phenylalanine (phe), and leucine (leu). Derivatized Thr and His residues co-eluted and are reported as a single peak. Under these conditions, asparagine and glutamine were converted to aspartic and glutamic acid during acid hydrolysis and have the highest racemization rates. However, the development of this method involved a careful choice of reagents and solvents as well as adjustment of the pH in order to minimize the rate of racemization.

Data were corrected for both the blank and for racemization after hydrolysis (according to Kaiser and Benner 2005), and are reported as the total concentration of dissolved combined amino acids in seawater (DCAA), the percent of UDOC that is amino acid carbon (%AA-UDOC), and as mole percentages (mol%) of individual amino acids. The coefficient of variation for DCAA between duplicate samples ranged from 0.7 to 4.6%; the relative standard deviation for the individual amino acids in each run was < 6%. It is possible that some amino acid peaks contained impurities, having significant implications for peaks with small areas. D-tyr peak areas were the smallest detected, but values were > 2 × blank (except for the deep N. Aegean sample, which we have omitted) and we interpret these data with caution.

2.8. Principal Components analysis

Principal components of amino acid and monosaccharide mol % data were determined using the Matlab statistics toolbox. Data were de-trended by removing the average and normalizing to the standard deviation for each variable prior to generating PCA data. Results are reported as PC loadings for individual amino acid or

monosaccharide mol % variables, PC scores of UDOM samples, and z-scores of principal components identified in the datasets.

3. Results and Discussion

The exchange of carbon between CO₂ and the ocean's large reservoir of DOC has substantial implications for global biogeochemical cycles and global climate. We still know little regarding the routes and fluxes of DOC production and remineralization, particularly in the meso- and bathypelagic ocean. DOC removal processes in the EMS may differ from those in the open ocean as bathypelagic temperatures are > 13 °C. Specifically, microbial remineralization processes that affect DOC concentration and/or composition in the meso- and bathypelagic Mediterranean waters may thus be more pronounced, and the chemical signatures of these processes may be more evident than in the major oceanic basins. For example, previous studies have noted the overwhelming presence of genes specific for the catabolism of amino acids and carbohydrates down to 4000 m (Martín-Cuadrado et al., 2007), and correlations between DOC and AOU have been shown to vary between water masses of the EMS (Seritti et al., 2003; Santinelli et al., 2010).

3.1. Water mass Characteristics and Distributions of bulk chemical and biological Parameters

Sample locations and hydrographic parameters are reported in Table 1. We identified the water masses sampled for UDOM according to their characteristic temperature and salinity signatures (Fig. 2), along with additional variables such as dissolved oxygen and inorganic nutrient concentrations (Tables 1 and 2). Specifically, we isolated UDOM from surface waters containing MAW or BSW, subsurface intermediate waters of the LIW, CIW, and TMW (200 to 750 m), and NAeDW, CDW, and EMDW from the deep E. Mediterranean Sea (1200 to 4350 m). Fig. 2b provides an enhanced view of the relations between the intermediate and deep water masses and types of the Aegean Sea. Note that the layer between 200 and 400 m in the North Aegean has similar characteristics to 1000-1400 m deep waters in the Cretan Sea. Also, the TMW and CIW waters seem to affect the shape of the T/S signature in the North Aegean.

AOU provides an estimate of the amount of oxygen consumed since a water parcel was at the surface and hypothetically in gaseous equilibrium with the atmosphere (i.e., fully saturated in oxygen). We observed significant variability in the AOU signature of water masses sampled in this study (Table 1), which may correspond to variability in the extent of removal of semi-labile DOC (Klein et al., 2003; Seritti et al., 2003; Santinelli et al., 2006). POC flux and the processes associated with that flux attenuation could also affect AOU, but the EMS is one of the well-known basins of low productivity of the world ocean; as such, organic particles are scarce in its sub-surface layers (Stavroulakis et al., 2006; Karageorgis et al., 2008). Thus, the oxidation of POC at depth could have had a minor effect on the levels of AOU and DOC, compared to that which occurs in more productive ocean basins. Water mass mixing definitely altered the concentration of both parameters and may have contributed to the observed variation in AOU and DOC concentrations. Sampling for both dissolved oxygen and DOC was performed simultaneously in the core of specific water masses that are characterized by different ages, sources, paths and hydrochemical properties. Thus each data pair may provide a signature of the specific history and path of the associated water mass.

Surface waters (0-100 m) in all sampling locations were close to oxygen saturation or even over-saturated, with AOU concentrations ranging between -8.9 and 33.3 μmol L⁻¹. Elevated AOU values were observed at depths > 200 m, reflecting the history of

Table 2
Inorganic and organic nutrients, and picoplankton abundance and activity at the different sampling sites and depths.

Station	Depth (m)	DIN ($\mu\text{mol L}^{-1}$)	DIP ($\mu\text{mol L}^{-1}$)	DON ($\mu\text{mol L}^{-1}$)	Picoplankton ($\times 10^5$ cells mL^{-1})	Picoplankton Activity ($\text{pmol leu L}^{-1} \text{h}^{-1}$)
N. Aegean	10	0.7	0.05	9.7	5.5	110.32
	200	1.9	0.08	6.6	1.6	4.91
	1000	4.6	0.15	4.9	0.6	2.09
S.W. Aegean	10	0.2	0.03	9.7	3.1	48.90
	500	1.2	0.06	5.3	1.2	4.05
	1200	3.9	0.16	5.1	0.6	1.52
Ionian	10	0.1	0.03	5.9	nd	27.13
	250	0.8	0.04	10.1	1.2	1.93
	750	3.1	0.15	6.0	0.4	0.10
	4350	4.0	0.15	7.1	0.3	1.16
S. Aegean	10	0.4	0.03	5.3	nd	69.33
	750	3.0	0.11	5.2	1	8.35
	1400	3.3	0.14	4.5	0.6	2.68

the different water masses occupying these layers. The highest AOU values ($61.7\text{--}68.2 \mu\text{mol L}^{-1}$) were recorded in the Ionian Sea, at depths 750–1000 m, representing the ‘aged’ TMW water mass (see above). The lower AOU ($49.4 \mu\text{mol L}^{-1}$) of the Levantine Intermediate waters, lying above the TMW layer, reveals its recent ventilation with respect to TMW. Below TMW, at the depth range from 2000 to 4350 m, the AOU values decrease gradually, implying that the deepest EMDW is probably younger (AOU of $49.0 \mu\text{mol L}^{-1}$) than the EMDW of the overlying layers (AOU of $58.2\text{--}53.4 \mu\text{mol L}^{-1}$). In the N. Aegean, the NAEADW, which has remained isolated since the major deep water formation event of winter 1993 (Zervakis et al., 2003), is characterized by high AOU, with values reaching $59.3 \mu\text{mol L}^{-1}$. In the South Aegean basin (Fig. 1), the AOU levels did not exceed $47.7 \mu\text{mol L}^{-1}$. The CIW signature was also detected at about 250 m depth in the South Aegean station from its low AOU ($16.9 \mu\text{mol L}^{-1}$), evidence of recent ventilation during the previous winter.

DOC ranged from 77 to $120 \mu\text{mol C L}^{-1}$ in surface waters where UDOM was collected (Table 1; avg. \pm sd = $93 \pm 18 \mu\text{mol C L}^{-1}$), and from 48 to 65 in subsurface waters (avg. \pm sd = $54 \pm 6 \mu\text{mol C L}^{-1}$). A negative correlation was observed between AOU and DOC for all samples with AOU > 0 collected during the POSEIDON cruise ($R^2 = 0.53$, $n = 33$, $p \ll 0.001$; Fig. 3). Based on estimates of the slope of this relationship and a molar respiratory quotient of 106/154 (Anderson and Sarmiento, 1994), Arístegui et al. (2002) determined that DOC accounted for < 10% of AOU in deep open ocean waters. In this study, we observe a $\Delta\text{DOC}/\Delta\text{AOU}$ value (\pm 95% confidence interval) of -0.19 ± 0.12 for waters where AOU > 0 (Fig. 3). To correct for changes in DOC due to mixing, potential temperature was included in this multiple regression analysis, according to Doval and Hansell (2000). DOC removal in the EMS thus accounts for $27 \pm 18\%$ of AOU and is higher than previous estimates for the global ocean (e.g., < 10%; Arístegui et al., 2002) and consistent with that observed for specific water masses of the Mediterranean Sea (Santinelli et al., 2010). This estimate is slightly higher than estimates of DOC respired during North Atlantic Deep Water formation (7–29%, Carlson et al., 2010) and is more similar to estimates at shallower depths in the open ocean (e.g., 15 to 41% at the BATS site; Hansell and Carlson 2001). This estimate includes samples collected from a variety of water masses in the subsurface EMS, thus yielding more variability than that reported for studies of $\Delta\text{DOC}/\Delta\text{AOU}$ along isopycnals (e.g., Doval and Hansell 2000). The mesopelagic and bathypelagic waters of the EMS are relatively warm (> 13°) and DOC rich ($48\text{--}65 \mu\text{mol C L}^{-1}$) compared to open ocean basins,

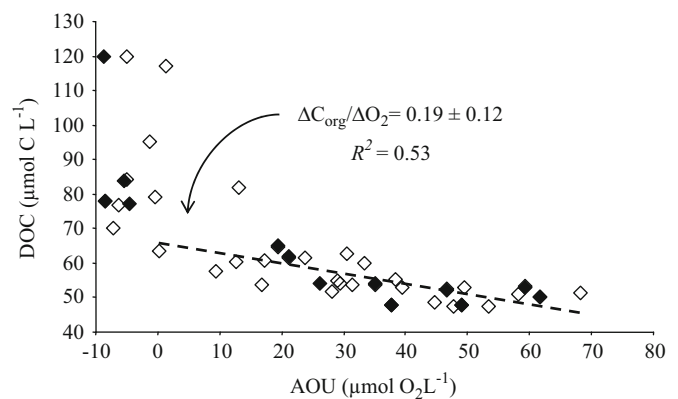


Fig. 3. AOU versus DOC for all stations of the POSEIDON cruise (open diamonds), and for stations where UDOM was collected (filled diamonds). The dashed line represents the regression for all stations where AOU > $0 \mu\text{mol L}^{-1}$.

and are thus likely to exhibit more efficient or extensive DOC respiration (Carlson et al., 2010).

Nutrient concentrations and picoplankton abundance and activity were also determined at depths where seawater was collected for UDOM isolation (Table 2). Dissolved inorganic nitrogen (DIN) and phosphorus (DIP) collected during the POSEIDON cruise exhibited profiles typical for the ultra-oligotrophic EMS, with surface concentrations ranging from below detection limits to $0.81 \mu\text{mol L}^{-1}$ and $0.05 \mu\text{mol L}^{-1}$, respectively, and increasing to $4.8 \mu\text{mol L}^{-1}$ and $0.16 \mu\text{mol L}^{-1}$, respectively, in subsurface waters (Table 2). The high subsurface DIN:DIP ratios (avg. \pm sd = 28 ± 4) agree with previous reports of the phosphorus-deficient EMS (Krom et al. 1992, Krasakopoulou et al. 1999).

The mean (\pm sd) abundance of picoplankton was $4.3 \pm 1.7 \times 10^5$ cells mL^{-1} in the surface and $8.3 \pm 4.4 \times 10^4$ cells mL^{-1} in subsurface waters. In general, at stations where UDOM was collected, *Bacteria* represented the bulk of picoplankton in both surface ($65 \pm 10\%$) and subsurface ($39 \pm 10\%$) waters (data not shown). Picoplankton abundance estimated by flow cytometry was well correlated with DOC (Fig. 4a, $R^2 = 0.67$, $n = 26$, $p \ll 0.001$). Some samples from the subsurface depths (ranging from 100 to 250 m) of the S. Aegean were above the general trend (circles). These outliers may be indicative of region-specific processes, such as the high dust-deposition event that occurred

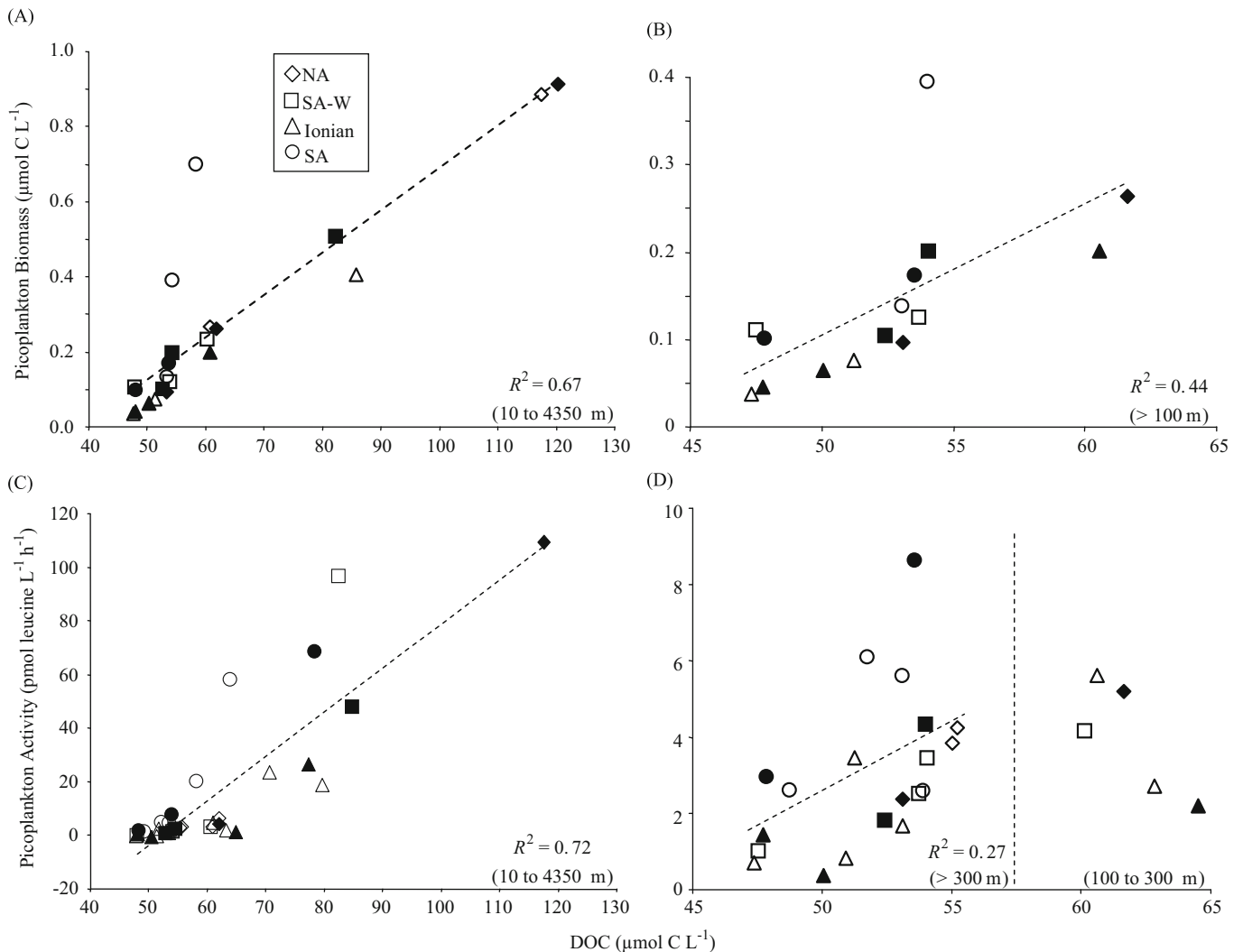


Fig. 4. DOC concentration versus (A & B) picoplankton abundance and (C & D) heterotrophic picoplankton activity observed during the POSEIDON cruise in the N. Aegean (NA, diamonds), Southwest Aegean (SA-W, squares), Ionian (triangles), and S. Aegean Seas (SA, circles). Filled symbols represent stations where UDOM samples were collected, and the dashed lines represent linear regressions that are statistically significant ($p < 0.05$) and include the entire datasets, except in (D), where the regression represents values below 300 m depth.

in this area during the sampling period. Picoplankton abundance was also well correlated with DOC at depths below 100 m (Fig. 4b, $R^2 = 0.44$, $n = 18$, $p < 0.005$). DOC was also well correlated with heterotrophic picoplankton activity (Fig. 4c, $R^2 = 0.72$, $n = 39$, $p \ll 0.001$). Fig. 4d is a plot of these variables below 100 m. There was a significant correlation at depths > 300 m ($R^2 = 0.27$, $n = 21$, $p < 0.02$), but samples at depths between 100 m and 300 m plotted below this trend.

Picoplankton carbon biomass comprised $< 0.8\%$ of bulk DOC, confirming that changes in picoplankton abundance alone cannot explain the observed variability in DOC. Sempéré et al. (2002) showed similar relationships between DOC and bacterial production in the Northern Aegean, attributing these trends to the enhancement of bacterial activity driven by input of DOC from the Black Sea. The close association between DOC stocks and picoplankton abundance and activity observed in this study is similar to those gradients found in estuarine and coastal aquatic systems (e.g. Wetzel, 1992; Fernandes et al., 2008), but is rare for marine systems (e.g., Carlson and Ducklow, 1995; Kaartokallio et al., 2007; H. Ducklow, pers. comm.). This tight coupling, together with the relationship between AOU and DOC, imply that heterotrophic remineralization processes exert a significant control on the cycling of DOC in these waters.

3.2. UDOM isolation and Correlations with AOU and the Picoplankton community

UDOM samples ($n = 17$) were concentrated with a spiral-wound filter of a nominal MWCO of 500 Da; DOC retention efficiencies are reported in Table 1. This system retained 65% of a 820 Da fluorescent compound (Alexa Fluor 594 dye) that was concentrated from 7 to 1.8 L. Fluorescence was intermittently detected in the permeate of the system, most notably during ultrafiltration of the first 3 L of solution (data not shown). The 500 Da cartridge filters processed pre-filtered seawater at approximately 30 L h^{-1} , and retained on average ($\pm \text{SD}$) $49 \pm 17\%$ of DOC in surface and subsurface seawater samples (Table 1). Amino acid analyses were performed on aliquots of UDOM at this stage. Subsequently, UDOM samples were diafiltered to remove salts, which also removed organic carbon and reduced the retention efficiency to an average ($\pm \text{SD}$) of $25 \pm 12\%$. These samples were then lyophilized and used for monosaccharide and $^1\text{H-NMR}$ characterization analyses. These analyses are discussed in further detail below.

The correlation between DOC and the picoplankton community was not paralleled by the UDOC pool. Also, there was no correlation between UDOC and total DOC, or with AOU. Together,

these observations suggest that *bulk* UDOC is not representative of the component of DOC that is coupled to the picoplankton community. While *bulk* UDOC was apparently unrelated to either AOU or picoplankton proxies for remineralization, *specific components* of UDOC did appear to be tightly coupled to both AOU and the microbial community (see below).

The variability in UDOC recovery reported in Table 1 (%DOC retained) is relatively high compared to previous ultrafiltration studies in the marine environment (e.g., Guo et al., 1996; Aluwihare et al., 1997; Benner et al. 1997). This result could be due to our use of a 500 Da membrane for ultrafiltration; to the authors' knowledge this study provides the first reports of the chemical characteristics of this fraction of DOM. As such, we are unable to determine if high variability in UDOC recovery is an artifact of sampling procedures or natural variability. We considered the possibility that UDOC recovery influenced the variability observed for each UDOM chemical composition parameter determined in this study. Indeed, one may expect that variability in the percentage of DOC that is > 500 Da, whether derived naturally or from sampling procedures, could yield substantial variability in the concentration and distribution of amino acids and monosaccharides in UDOM. Despite this concern, only the heteroatom ¹H-NMR resonances showed a slightly significant correlation with variability in UDOC recovery ($r = -0.55$, $p = 0.05$). Other correlations with UDOC recovery, or lack thereof, are presented throughout the manuscript. If insufficient sampling protocols resulted in variability in UDOC recovery and altered the chemical composition between samples, the strong correlations between UDOC-specific chemical composition measurements and independent measurements of other site-specific parameters reported below are a remarkable coincidence.

To further examine the UDOM chemical composition of the various water masses, we determined ¹H-NMR spectra as well as amino acid and monosaccharide concentrations and relative mole distributions. The data were sorted according to the AOU value of the corresponding water masses to assess the correlation between UDOM chemical composition and AOU (Tables 3 and 4). Comparisons of UDOM composition in this study are drawn between samples that were 1) isolated during the POSEIDON cruise and analyzed prior to diafiltration for amino acid

characterization, or 2) isolated during either the POSEIDON or SESAME cruises and analyzed after diafiltration for carbohydrate and ¹H-NMR characterization. While these data likely represent different fractions of bulk DOM, no comparisons are drawn between these fractions unless otherwise noted.

3.3. UDOM ¹H-NMR characterization

Selected ¹H-NMR spectra are shown in Fig. 5 and the relative contribution of aliphatic (0.5 to 1.8 ppm), alpha-substituted (1.8 to 3.2 ppm), and heteroatom-substituted resonances (3.2 to 4.6 ppm) in all UDOM samples are reported in Table 3 alongside carbohydrate data. ¹H-NMR spectra were dominated by characteristic aliphatic, alpha-substituted (acetate), and heteroatom-substituted resonances, and trends in the relative abundance of these resonances were similar to previous reports (e.g., Aluwihare et al., 2002). In general, UDOM from higher AOU waters (i.e., subsurface UDOM) exhibited ¹H-NMR spectra with proton abundance evenly distributed as broad peaks among all resonances, while ¹H-NMR spectra of UDOM isolated in low AOU waters were dominated by the heteroatom-substituted (likely carbohydrate) resonances. Aliphatic and alpha-substituted resonances were significantly correlated with AOU ($r = 0.73$ and 0.92 , respectively, $p < 0.005$; Table 3). Heteroatom-substituted resonances were significantly and inversely correlated with AOU ($r = -0.85$, $p < 0.001$). UDOM collected from the N. Aegean basin (1000 m) exhibited a ¹H-NMR spectrum similar to that observed for surface samples dominated by heteroatom-substituted resonances (Fig. 5, Table 3). This anomalous sample was excluded from the UDOM comparisons in this section and from those discussed below, unless otherwise noted.

3.4. UDOM carbohydrate composition

Monosaccharide abundances and distributions in UDOM are reported in Table 3 and are sorted according to the AOU value of the corresponding water mass. DCNS ranged from 0.4 to 3.8 $\mu\text{mol C L}^{-1}$, representing 2 to 24% of UDOC (Table 3); these

Table 3
Monosaccharide mol % distributions, and % contribution of ¹H-NMR regions to spectra of UDOM, sorted by AOU values of waters where seawater was collected. Bold values indicate a significant correlation (r) between AOU and monosaccharide mole % or ¹H-NMR component data as defined by the Pearson correlation coefficient. *nd* = no data.

Station	Depth (m)	AOU ($\mu\text{mol L}^{-1}$)	DCNS ($\mu\text{mol C L}^{-1}$)	%NS-UDOC	Monosaccharide mole percentages							¹ H-NMR group			
					rham	fuc	arab	xyl	mann	glu	gal	aliphatic	alpha subs	hetero subs	
DB2-Athos	2	-8.624	<i>nd</i>	<i>nd</i>	<i>nd</i>	<i>nd</i>	<i>nd</i>	<i>nd</i>	<i>nd</i>	<i>nd</i>	<i>nd</i>	<i>nd</i>	32	28	41
W. Cretan	2	-5.393	<i>nd</i>	<i>nd</i>	9.4	11.6	5.8	8.7	15.5	20.2	28.8	<i>nd</i>	<i>nd</i>	<i>nd</i>	<i>nd</i>
Ionian	2	-4.628	<i>nd</i>	<i>nd</i>	8.7	11.1	6.7	9.4	15.9	19.2	29.0	<i>nd</i>	<i>nd</i>	<i>nd</i>	<i>nd</i>
DB8-Cretan	2	-8.843	<i>nd</i>	<i>nd</i>	12.3	11.9	6.4	5.7	17.8	17.7	28.2	<i>nd</i>	<i>nd</i>	<i>nd</i>	<i>nd</i>
Sesame NS1	2	-4.99	1.6	9.1	9.3	12.4	5.6	8.3	14.9	21.3	28.1	25	26	49	
Sesame NS6	2	-1.28	3.7	14.3	9.1	11.7	5.6	7.2	17.7	15.9	32.7	27	29	44	
KM3NET C2	2	<i>nd</i>	3.8	24.3	10.2	12.2	6.4	6.9	16.6	19.7	28.0	27	30	44	
Ionian	250	19.323	2.5	10.4	9.4	11.1	6.4	5.3	17.2	21.7	28.8	33	32	35	
DB2-Athos	200	21.109	0.5	2.6	10.2	10.8	5.9	5.9	20.1	20.4	26.7	33	33	34	
W. Cretan	500	26.256	0.6	2.9	15.0	14.6	6.1	6.0	15.3	20.3	22.8	34	34	33	
DB8-Cretan	750	35.161	0.5	4.6	12.7	12.6	6.7	6.7	16.1	20.1	25.0	33	34	33	
DB8-Cretan	1350	37.823	0.4	4.3	12.3	9.2	6.9	5.6	19.2	19.8	27.0	34	35	31	
W. Cretan	1200	46.675	0.5	2.3	10.8	11.3	5.7	5.1	20.7	21.7	24.6	35	35	31	
Ionian	4350	48.953	1.9	7.7	12.9	14.2	5.9	9.9	16.4	22.1	18.7	33	33	34	
DB2-Athos	1000	59.296	<i>nd</i>	<i>nd</i>	9.5	11.5	5.9	6.3	17.4	24.2	25.2	28	30	42	
Ionian	750	61.703	<i>nd</i>	<i>nd</i>	11.1	10.8	9.0	8.2	16.9	20.7	23.2	34	35	31	
r (AOU)	-	-	-0.56	-0.63	0.49	0.01	0.50	-0.12	0.32	0.54	-0.76	0.73	0.92	-0.85	
p	-	-	0.092	0.069	0.075	0.973	0.069	0.683	0.265	0.046	0.002	0.003	< 0.001	< 0.001	

Table 4
Amino acid abundance and mol % distributions in UDOM, sorted by AOU values of waters where seawater was collected. Bold values indicate a significant correlation (*r*) between AOU and amino acid mole % data as defined by the Pearson correlation coefficient.

Station	Depth (m)	AOU ($\mu\text{mol O}_2 \text{ L}^{-1}$)	DCAA (nmol L^{-1})	%AA-UDOC	asx	D-asx	glix	D-glix	ser	D-ser	thr/his	gly	arg	ala	D-ala	tyr	D-tyr	val	phe	leu
DB2	2	-8.624	461	1.6	12.7	2.6	9.0	2.0	5.5	1.5	8.2	33.0	2.5	8.8	3.1	2.6	0.4	3.6	0.8	3.8
WC	10	-5.393	581	1.4	14.0	3.9	8.6	2.7	3.9	2.1	5.6	32.2	3.6	8.0	4.4	2.7	0.4	3.2	1.3	3.4
DB2	200	21.109	216	1.2	12.7	4.6	8.2	2.6	3.6	2.1	5.3	36.4	2.9	8.0	4.4	2.2	0.5	3.1	0.3	3.2
WC	500	26.256	334	1.1	10.5	5.1	8.8	2.7	4.1	2.9	5.7	36.4	1.8	7.7	4.9	2.4	0.6	2.4	1.3	2.5
WC	1200	46.675	202	0.9	12.1	6.2	10.4	3.0	2.2	1.7	3.4	36.6	3.5	7.2	5.1	2.1	0.3	2.8	0.7	2.6
Ionian	4350	48.953	356	1.0	13.2	5.1	9.7	2.9	2.3	1.3	3.7	34.7	3.9	8.1	4.4	1.8	0.2	3.6	1.4	3.7
DB2	1000	59.296	188	0.9	14.5	3.2	9.6	1.6	3.0	1.0	5.4	33.6	3.5	9.0	2.3	2.1	0.2	4.4	1.7	5.0
Ionian	750	61.703	270	0.8	12.3	5.8	9.1	3.4	2.2	1.6	3.3	37.1	3.9	8.0	4.4	1.8	0.3	2.8	1.0	2.9
		<i>r</i> (AOU)	-0.73	-0.98	-0.31	0.89	0.55	0.84	-0.90	-0.24	-0.89	0.80	0.47	-0.55	0.57	-0.95	-0.48	-0.33	0.12	-0.49
		<i>p</i>	0.063	< 0.001	-	0.007	-	0.02	0.003	-	0.007	0.031	-	-	-	0.001	-	-	-	-

carbohydrate yields are consistent with previous reports (e.g., Aluwihare et al., 2002; Benner, 2002). Both DCNS and %NS-UDOC were correlated with $^1\text{H-NMR}$ aliphatic, alpha-substituted, and hetero-atom substituted resonances ($r = -0.69, -0.61,$ and $0.67,$ respectively; $p < 0.05$), and generally showed increased concentrations in surface waters but were not significantly correlated with AOU or picoplankton activity. Relative mole percentages (mol %) of galactose (avg. \pm sd = $26.4 \pm 3.4\%$), glucose ($20.4 \pm 1.9\%$), and mannose ($17.2 \pm 1.7\%$) were consistently high in all UDOM samples; this latter observation is unique to this sample set as mannose typically exhibits lower relative mol % in UDOM (e.g., 10 to 16%; McCarthy et al., 1996; Aluwihare et al., 2002). In general, UDOM isolated for this study exhibited a monosaccharide composition consistent with previous UDOM reports even though it likely includes relatively more of the LMW pool of DOM

AOU was significantly correlated with mol % of glucose ($r = 0.54, p < 0.05$) and was significantly and inversely correlated with mol % of galactose ($r = -0.76, p < 0.005$). No other monosaccharide mol % was correlated with AOU. The significant correlations observed for glucose and galactose with AOU imply that these monosaccharides vary inversely during the apparent degradation of semi-labile UDOM, or other processes that contribute to increase the AOU of a water mass. These observations are similar to previous reports of galactose and glucose variability in seawater (e.g., McCarthy et al., 1996; Skoog and Benner, 1997; Amon and Benner, 2003; Goldberg et al., 2009).

Similar to previous studies, carbohydrates were a relatively small fraction of bulk DOC ($< 4 \mu\text{mol C L}^{-1}$) and thus represented only a small fraction of the change in DOC or AOU between surface and deep waters. Thus, the observed correlations between monosaccharide distributions and AOU may not be a direct representation of the removal semi-labile DOC in subsurface waters. That is, the standing stock of non-carbohydrate UDOC removed as AOU increases far exceeds that of carbohydrate UDOC; observed changes in monosaccharide distributions may thus be complementary to this flux. Rather than representing the effects of selective preservation or consumption of a semi-labile carbohydrate component, monosaccharide distributions may reflect transient fluxes of monosaccharides in UDOM that become more important in the deep ocean.

3.5. UDOM Amino acid composition

Amino acid concentrations and mole distributions were determined for 8 UDOM samples before diafiltration; samples were sorted according to AOU values and data are shown in Table 4. In general, the UDOM isolated in this study represents a greater fraction of bulk DOM than previous UDOM reports and the composition of this pool may exhibit signatures more closely related to LMW DOM than previous UDOM composition studies. For example, Kaiser and Benner (2009) report lower yields of amino acids and relatively depleted abundances of hydrophobic amino acids in LMW DOM compared to HMW DOM. In this study, the concentrations of DCAA ranged from 51 to 158 nmol L^{-1} (188 to 581 nmol C L^{-1}) in surface and subsurface waters. Glycine was by far the most abundant amino acid in all UDOM samples, representing $35.0 \pm 1.9\%$ (avg. \pm sd) of all amino acids, followed by aspartic acid ($12.4 \pm 1.1\%$), glutamic acid ($9.0 \pm 0.7\%$), and alanine ($8.1 \pm 0.6\%$). Amino acids in UDOM represented $41 \pm 11\%$ of amino acids measured in bulk seawater samples (thus a significant amount is present in the HMW fraction); and bulk seawater samples showed similar mole distributions, except for significantly higher relative abundances of alanine ($14.3 \pm 3.5\%$, $p < 0.001$) and serine ($7.4 \pm 3.9\%$, $p < 0.005$, data not shown).

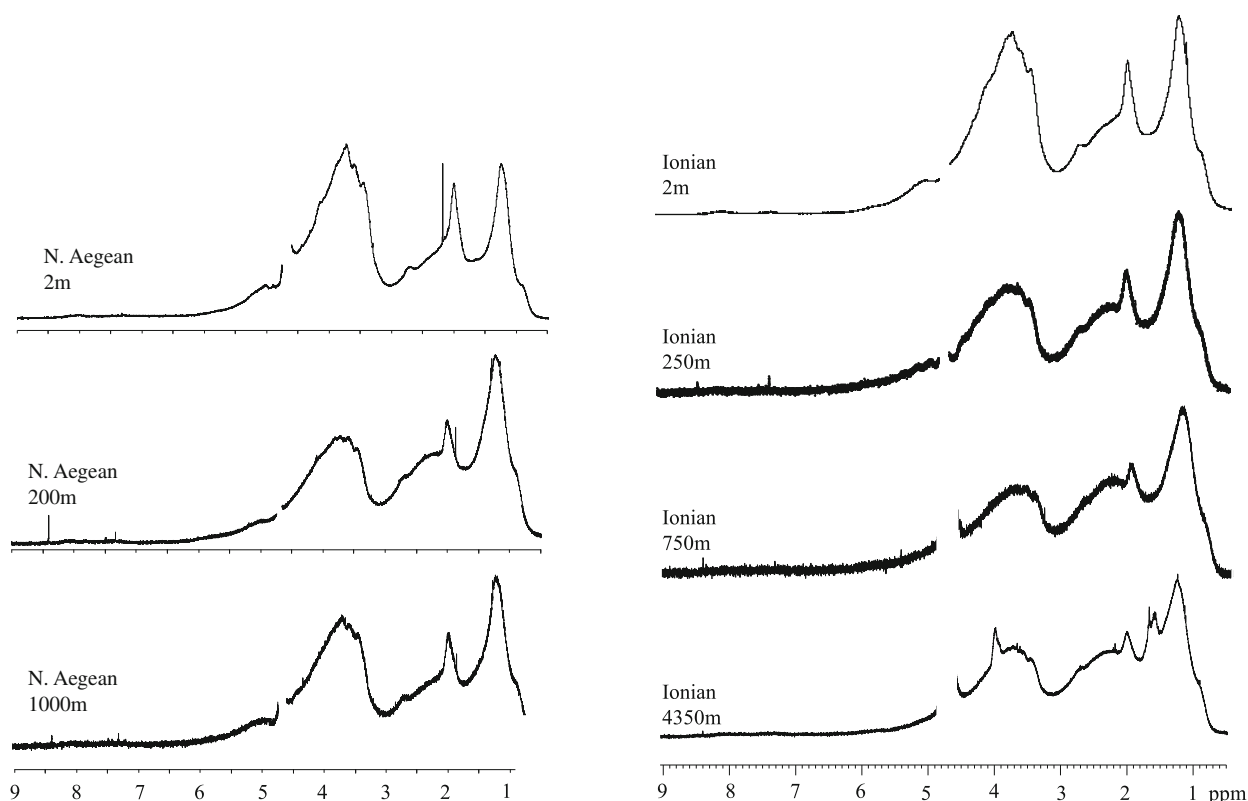


Fig. 5. Characteristic UDOM $^1\text{H-NMR}$ spectra at various depths of the North Aegean and Ionian Seas. Sample names are provided for each spectrum; the HDO peak at 4.7 ppm was removed from all spectra.

Several amino acids were below the detection limit in bulk seawater samples and were not considered in mole distribution comparisons. The range in DCAA observed in this study is lower than that reported for UDOM in the open ocean (178 to 278 nmol L^{-1} ; McCarthy et al. 1996). However, the relative distributions (mol%) of amino acids in UDOM agree with previous reports, as does the fraction of amino acids in UDOM relative to the total pool of amino acids determined in bulk seawater samples (Aluwihare and Meador 2008, and references therein). The amino acid carbon contribution to UDOC (%AA-UDOC) ranged from 0.83 to 1.61% and was lower than previous reports (~ 3 to 6%; Benner et al., 2002; Aluwihare and Meador, 2008); the error of this value was $< 0.03\%$ for all samples.

The average (\pm sd) enantiomeric ratios (D/L) of aspartic acid (0.39 ± 0.11) and alanine (0.56 ± 0.11) were similar to the averages in the open ocean (0.42 and 0.49, respectively; Pérez et al., 2003) and in UDOM (0.37 and 0.50, respectively; McCarthy et al., 1998). The D/L ratios for serine (0.60 ± 0.17) and glutamic acid (0.30 ± 0.05) appear to be enriched in the D-enantiomer compared to previous reports (0.09 and 0.15, respectively; Pérez et al., 2003). McCarthy et al. (1998) report a D/L ratio for tyrosine of 0.10, which was not much higher than the racemization blank reported for that study, and lower than observed in this study (0.17 ± 0.05). The enantiomeric amino acid ratios determined in this study were corrected for hydrolysis-related racemization according to Kaiser and Benner (2005), whereas the previous reports serving as comparisons did not apply this correction. Our uncorrected enantiomeric data were not significantly different from the corrected data, maintaining the same relationship as the comparisons noted above.

The UDOM sample collected in the deep N. Aegean basin (1000 m) was not included in the computations above or those in the preceding amino acid discussion. The composition of this

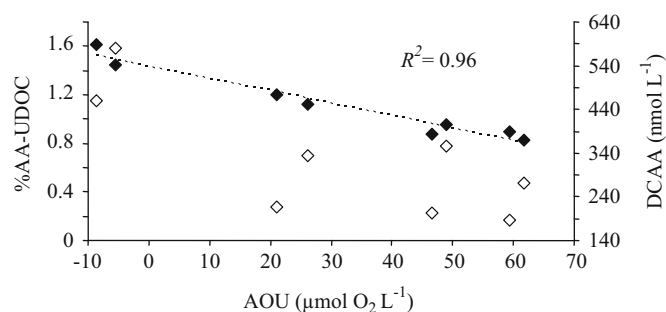


Fig. 6. AOU versus %AA-UDOC (filled symbols) and DCAA concentration (open symbols). The dashed line represents linear regression of the %AA-UDOC data.

deep ocean sample was remarkably similar to samples collected in the surface ocean, particularly in regard to its $^1\text{H-NMR}$ spectra (Fig. 5) and low D-amino acid content (Table 4). This sample also exhibited the lowest UDOC (21 μM ultrafiltered, 5 μM diafiltered; Table 1). These characteristics may result from the unique ventilation patterns of the N. Aegean basin, where the rapid deep water formation and reduced mixing presumably could have affected the chemical composition of UDOM. Additionally, prior to deep water formation, these waters likely contained alloctonous inputs of DOM from the Black Sea that may differ in chemical composition from that produced in the EMS. These findings provide additional evidence that North Aegean deep waters differ from the rest of the EMS deep water masses due to a long stagnation period from 1994 to at least 2007 (our sampling year), during which there has been low or no ventilation (Zervakis et al., 2003; Zervakis and Krasakopoulou, unpublished data).

3.5.1. Amino Acids and AOU

Assessing the correlation between AOU and the amino acid composition of UDOM allowed us to examine the chemical transformations of DOM that may accompany increases in AOU, which seemingly represents the degradation of semi-labile DOC. Significant correlations between AOU and %AA-UDOC and mole distributions are shown in bold in Table 3. AOU and %AA-UDOC were significantly and inversely correlated ($r = -0.98$, $p < 0.001$, Fig. 6). DCAA showed a similar but less significant correlation with AOU ($r = -0.74$, $p = 0.063$, Fig. 6). It thus appears that %AA-UDOC integrates a multitude of processes that are coupled to AOU but are not represented by DCAA alone. While there was a strong correlation between %AA-UDOC and AOU (Fig. 6), amino acid carbon normalized to bulk DOC shows no correlation with AOU ($r = 0.16$, data not shown). The amino acid signature that accompanies changes in AOU is thus only evident in the dynamics of UDOC, and presumably, associated with the HMW fraction of bulk DOC. Given that the ultrafiltration sampling procedures did not affect AOU measurements, the correlation between AOU and %AA-UDOC provides convincing evidence that the range in UDOC recovery reported in Table 1 records natural variability.

The increase in %AA-UDOC in low AOU waters is likely due to local production by marine autotrophs in the surface ocean (e.g., Hubberten et al., (1994), an amino acid source that is absent from high AOU waters in the subsurface ocean. Table 4 also reveals that UDOM mole percentages of D-asp, D-glu, and gly were significantly correlated with AOU ($r = 0.89$, 0.84 , and 0.80 , respectively; $p < 0.05$), and ser, thr/his, and tyr were significantly and inversely correlated with AOU ($r = -0.90$, -0.89 , and -0.95 , respectively; $p < 0.01$). Some of these significant differences were observed in previous reports of amino acid distributions in the marine environment, which have generally noted increased concentrations of alanine and glycine, and decreased concentrations of hydrophobic amino acids (e.g., leucine, phenylalanine, valine) in “more degraded” DOM (e.g., Yamashita and Tanoue, 2003). In this study, the sum of the total carbon-normalized D to L-enantiomeric amino acids in UDOM (Σ -D/L) ranged from 0.23 to 0.44. Σ -D/L of UDOM was significantly correlated with AOU ($r = 0.77$, $p < 0.05$) and was primarily driven by changes in D-asp and D-glu (Table 4). These amino acids also appeared to increase with depth; this observation contrasts that observed by McCarthy et al. (1998) in the North Atlantic and Pacific basins and may be due to the higher recovery of UDOM examined in this study or differences in the subsurface regions of the EMS versus the open ocean. The dynamics of D-amino acids are further discussed below.

In this study, amino acids accounted for less than 2% of UDOC and less than 0.2% of bulk DOC ($< 0.6 \mu\text{mol C L}^{-1}$). As above for carbohydrates in seawater, the addition and removal of the $< 0.6 \mu\text{mol C L}^{-1}$ fraction of amino acid carbon cannot account for the large changes observed in AOU. Thus, the correlation between amino acid distributions and AOU may not directly reflect which of the amino acids were preferably removed or preserved as semi-labile UDOM is degraded, but may represent transient fluxes of amino acids in UDOM that vary with increasing AOU. For example, Pérez et al. (2003) speculated that the shift in the bacterial uptake ratios of D/L-amino acids from the surface to the mesopelagic zone of the N. Atlantic may reflect a shift in the production of bioavailable D/L-amino acids.

3.5.2. Amino Acids and picoplankton

Similar to trends observed with AOU, picoplankton community parameters were also significantly correlated with %AA-UDOC (Fig. 7) and were not correlated with DCAA. In order to assess the relationships between amino acid and picoplankton parameters,

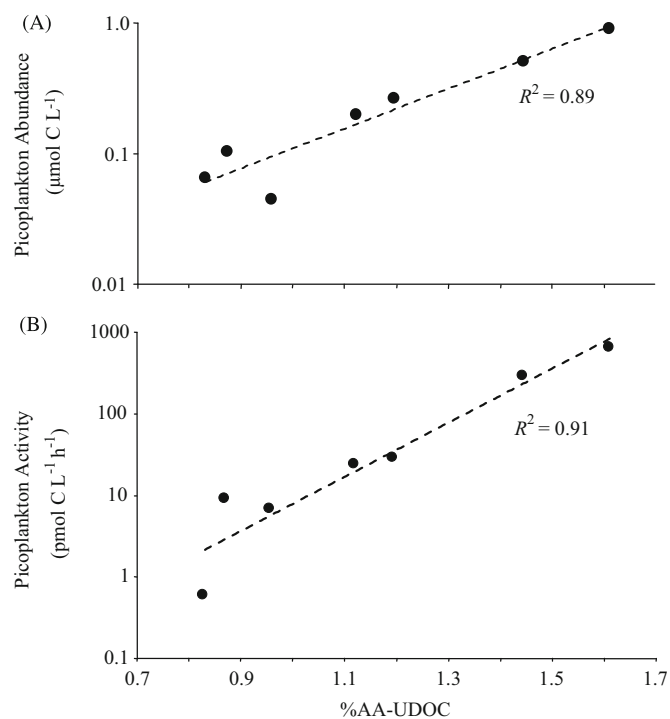


Fig. 7. Relationship between %AA-UDOC vs. picoplankton abundance (A) and picoplankton activity (B). Note picoplankton abundance and activity are plotted on a logarithmic scale. Dotted lines represent exponential regressions that were statistically significant ($p < 0.002$).

it is necessary to consider the inherent intracellular protein component that comprises a substantial portion of the microbial biomass. The measured carbon concentrations of amino acids in UDOM and those calculated for the picoplankton community (assuming $2 \times 10^{-14} \text{ g C cell}^{-1}$, an overestimate for the purpose of this comparison; Fukuda et al., 1998) are of the same order of magnitude ($\sim 10^{-7} \text{ mol C L}^{-1}$); however, there was no significant correlation between these parameters. These measurements thus appear to be exclusive, and the reported DCAA concentrations (in UDOM) are in fact measures of amino acids in the dissolved pool and do not include picoplankton biomass. Therefore, the correlations observed between amino acid and microbial parameters in Fig. 7 reflect the distinct variability of UDOM composition or the picoplankton community.

Estimates of %AA-UDOC appear to be significantly correlated with both picoplankton abundance and cell specific picoplankton activity (Fig. 7a, b; $R^2 > 0.89$, $p < 0.002$; note that the y-axis is a log scale). The relationship shown in Fig. 7a suggests that the proportion of amino acids in UDOC, while $< 2\%$ of UDOC, is tightly coupled to picoplankton abundance. Because count-estimated picoplankton abundance in deep waters may include dormant cells, the significant relationship between %AA-UDOC and picoplankton activity (Fig. 7b) provides more convincing evidence that amino acids in UDOM are coupled to the picoplankton community. This relationship also applies when considering only the metabolically slow dark ocean regions (i.e., those samples with %AA-UDOC $< 1.3\%$ in Fig. 7). DCAA was not correlated with picoplankton activity or abundance, or with AOU (Fig. 6).

Picoplankton activity and AOU are clearly associated with different timescales of turnover of organic matter (hours versus years), yet are related as increases in AOU record the cumulative effects of heterotrophic activity, and this metabolic activity becomes energetically constrained and decreases as a water mass ages (e.g., Hoehler, 2004). Fig. 6 and Fig. 7 show that %AA-UDOC is

strongly correlated with both AOU and picoplankton activity, but it is unclear whether: 1) %AA-UDOC mimics the relationship between DOC and AOU (Fig. 3) and also records the accumulative effects of heterotrophic activity over long timescales (i.e., more bioavailable amino acid components are removed and refractory components remain); or 2) changes in %AA-UDOC are manifested more rapidly, in equilibrium with reduced picoplankton activity.

The latter explanation is supported by the lack of correlation between DCAA and AOU or picoplankton activity (Figs. 6 and 7). If the former explanation was valid we would expect that DCAA would track AOU, similar to bulk DOC (Fig. 3), as the bioavailable components of UDOM set in the surface ocean are gradually removed. Also, the magnitude of the stocks of picoplankton and amino acids ($\sim 10^{-7}$ mol C L⁻¹) are similar, whereas that required to account for the AOU signal is much larger ($\sim 10^{-5}$ mol C L⁻¹). Further investigation of the co-variability between individual amino acid mole distributions and the picoplankton community are considered below.

3.6. Principal component analysis (PCA) of UDOM

Several indices assess the degree of degradation of organic matter; these are based on trends in monomer composition (e.g., Dauwe et al., 1999; Amon et al., 2001; Amon and Benner 2003) or make use of biomarkers to estimate the contribution of bacteria to

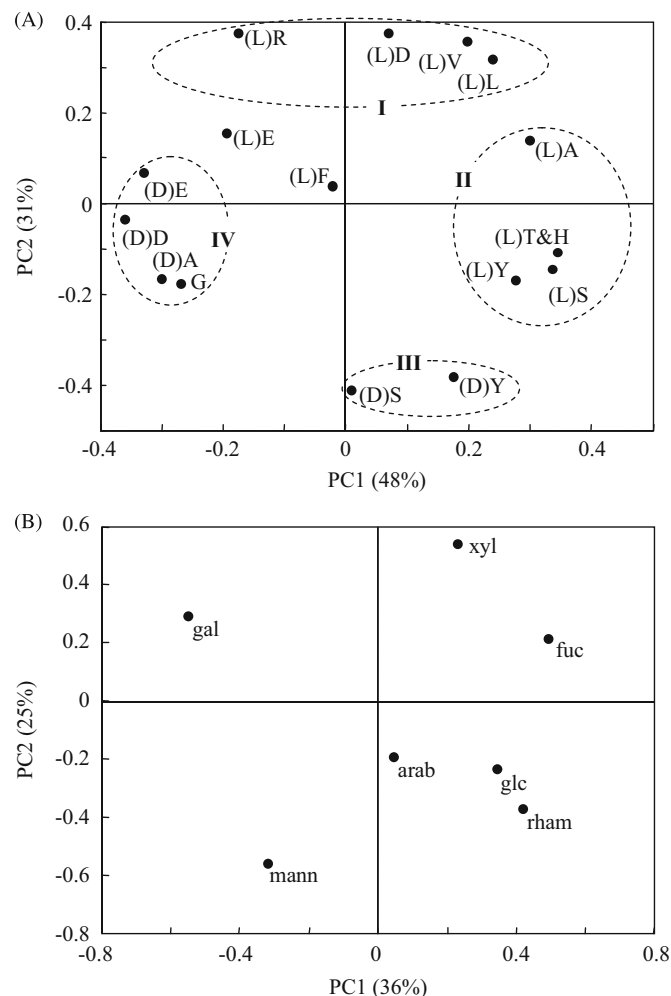


Fig. 8. Biplots of PC1 (x-axis) and PC2 loadings (y-axis) of (A) amino acid and (B) monosaccharide distributions in UDOM. Amino acids that plot in clusters identified in (A) are defined in the text.

DOM (e.g., McCarthy et al., 1998; Kaiser and Benner, 2008). These strategies interpret the composition of DOM in the parlance of amino acid or monosaccharide composition. AOU is a more direct proxy for remineralization of organic matter and is correlated to DOC stocks (Fig. 3); we assessed UDOM molecular level composition as it relates to this signal above (Tables 3 and 4). PCA identifies the axes that capture the greatest amount of variability within the sample set and thus presents an alternative framework to compare variability in UDOM composition. We used PCA to examine the variability in both amino acid and monosaccharide distributions in UDOM, similarly to Dauwe et al. (1999) who characterized diagenetic trends of sedimentary organic matter. However, the PCA analysis in this study considered several biogeochemical proxies, in addition to those related to diagenesis, in order to establish correlations with the axes that explain the majority of variability in molecular level composition.

PC1 and PC2 accounted for 48% and 31% of the variability in amino acid mol %, and 36% and 25% of monosaccharide mol % variability, respectively. Factor loadings for PC1 and PC2 of individual amino acids and monosaccharides are plotted in Fig. 8; amino acids or monosaccharides that cluster together vary similarly among UDOM samples. Also, PC1 and PC2 scores were generated for individual UDOM samples for both the amino acid and monosaccharide PCA (data not shown); these scores sort UDOM samples along the first and second principal component axes of compositional variability. PC scores were compared to additional biogeochemical data determined for each UDOM sample or sampling station. Significant correlations are reported in Table 5 and are sorted according to parameters that generally increase or decrease with depth. Thus, the information provided by PCA allowed us to distinguish the covariability between individual amino acids and monosaccharides within UDOM and the covariability between UDOM molecular composition and multiple site-specific parameters (in addition to the AOU comparisons above). The UDOM sample collected in the deep N. Aegean basin (1000 m) was not included in PCA for the reasons described above.

3.6.1. Amino acid PCA

The PC1 and PC2 loadings derived for each amino acid were used to sort amino acids into clusters, such that amino acids with similarly high loadings for either the PC1 or PC2 axis were grouped together (Fig. 8a). Amino acid clusters are identified as:

- Cluster I – arginine, L-aspartic acid, leucine, and valine
- Cluster II - L-alanine, L-serine, L-tyrosine, and the threonine and histidine peak
- Cluster III - D-serine and D-tyrosine
- Cluster IV - D-alanine, D-aspartic acid, D-glutamic acid, and glycine

Phenylalanine and L-glutamic acid were not sorted into groups because the PC1 and PC2 loadings for these amino acids were relatively low.

This amino acid PCA analysis is similar to that reported by Yamashita and Tanoue (2003) for amino acids in coastal and open-ocean DOM. Clusters II and IV exhibit high but opposite loadings for PC1. Clusters I and III have high and opposite loadings for PC2. These data indicate that variability of amino acids clusters II and IV are inversely proportional and best described by PC1, and any parameters correlated with PC1 are also likely correlated with the distribution of these amino acids. Similarly, parameters that are correlated with PC2 are likely correlated with amino acids in clusters I and III. The trends observed in this study are difficult to

Table 5

Correlations of site-specific physical, chemical, and biological parameters with PC1 and PC2 scores derived from PCA of amino acid or monosaccharide mol %. Parameters are grouped according to those that exhibit trends that generally decrease with depth (I), increase with depth (II), or unrelated with depth (III). Z-scores for individual PC are shown in parentheses. Correlations with amino acid concentrations are also shown. All reported correlations are significant to at least $p < 0.05$.

	DCAA	Variability in AA mole distribution		Variability in monosaccharide mole distribution		
		PC1 (48%)	PC2 (31%)	PC1 (36%)	PC2 (25%)	
I	Temperature	0.88	0.79	–	–	
	TOC	–	0.91	–	0.75	
	UDOC	–	–	–	–	
	DCAA	na	–	–	0.96	
	DCNS	–	–	–	0.66	
	%AA-UDOC	–	0.96	–	–	
	%NS-UDOC	–	–	–	–	
	¹ H hetero-subst	–	0.98	–	0.85	
	Cells mL ⁻¹	–	0.93	–	–	
	Pico. activity	–	0.89	–	–	
	Eubacteria	0.74	–	–	–	
II	Salinity	–	–0.80	–	–0.57 ^b	
	σ_t	–	–0.87	–	–0.79 ^b	
	AOU	–	–0.90	–	–0.67 ^b	
	Nitrate + Nitrite	–	–0.83	–	–	
	Phosphate	–	–0.84	–	–	
	DIN:DIP	–0.79	–0.79	–	–	
	Σ -D/L	–	–0.83	–	–	
	¹ H aliphatic	–	–0.91	–	–0.85	
	¹ H alpha-subst	–	–0.97	–	–0.83	
III	%DOC retained ^a	–0.07	–0.62	0.25	0.44	–0.23

^a Correlation was determined to examine if UDOC recovery influenced variability in amino acid or monosaccharide distribution. Non-diafiltered UDOC recoveries are used for comparisons related to amino acid analysis and diafiltered UDOC recoveries are used for comparisons of monosaccharide analysis. For all r reported, $p > 0.1$

^b These correlations were significant ($p < 0.05$) but the relationships were driven by surface samples with low salinity and AOU.

compare to those observed in Yamashita and Tanoue (2003) because we did not measure the same suite of amino acids (e.g., D-enantiomers are not reported in their study); however, these authors report similar relationships between glycine and the hydrophobic amino acids valine and leucine for PC1, as well as the similarly high loadings for arginine and L-aspartic acid for PC2.

The first principal component of variability in amino acid distribution (i.e., PC1) was significantly correlated with %AA-UDOC ($r = 0.96$, $p < 0.001$), but was not significantly correlated with DCAA or with %DOC retained by ultrafiltration. From this observation we can deduce that variability in amino acid mol % distribution was 1) more significantly coupled to the protein component of UDOM and not bulk amino acid concentrations in seawater, and 2) not an artifact of sampling procedures that may have altered retention of UDOC. A similar correlation with PC1 and %AA-UDOC was observed by Amon et al. (2001) and Yamashita and Tanoue (2003), which led these authors to suggest that degradation was the principal component driving the variability within their datasets. PC1 was also correlated with picoplankton abundance and activity ($r = 0.93$ and 0.89 , respectively; $p < 0.005$), and inversely correlated with AOU ($r = -0.90$, $p < 0.01$) and Σ -D/L ($r = -0.83$, $p < 0.02$; Table 5). PC1 thus captures the variability that was addressed in Sections 3.5.1 and 3.5.2 above, which used a more obtuse analysis of amino acid distributions, and indicates that D- amino acids in cluster IV are among the most variable amino acids in UDOM.

PC1 of amino acid mol % distribution was also significantly correlated with other UDOM composition measurements, including aliphatic, alpha-substituted, and heteroatom-substituted regions of UDOM ¹H-NMR spectra ($r = -0.91$, -0.97 , and 0.98 , respectively; $p < 0.005$) and several other parameters that are associated with water mass age or depth-related trends in the water column (Table 5). This observation indicates that changes in UDOM ¹H-NMR spectra are accompanied by changes in the mol %

signature of amino acids in UDOM; in particular, those amino acids with high absolute loadings for PC1 (i.e., clusters II and IV, Fig. 8A). The amino acids D-asx, D-glx, gly, and D-ala (cluster IV, with largely negative PC1 loadings) are relatively more abundant in UDOM with ¹H-NMR spectra exhibiting higher aliphatic and alpha-substituted resonances; ala, leu, val, phe, and asx (cluster II, with high PC1 loadings) are more abundant in UDOM with ¹H-NMR spectra exhibiting higher heteroatom substituted resonances. Again, amino acids are a small fraction of UDOC and these amino acids have similar abundances of aliphatic, alpha-substituted, and heteroatom substituted protons (if anything the cluster II amino acids would have relatively more aliphatic protons); therefore the amino acid distributions are not directly driving the observed variability in ¹H-NMR spectra. Variability in amino acid mol % and ¹H-NMR resonances do appear to be impacted by the same, unidentified, principal component however. As noted above, the diafiltered sample used to determine ¹H-NMR spectra contained a smaller portion of the total DOC pool than that used for amino acid measurements, and it is possible that the DOM lost during diafiltration (in preparation for ¹H-NMR analysis) was enriched in cluster IV amino acids as well as aliphatic and alpha-substituted resonances, or relatively depleted in cluster II amino acids and heteroatom-substituted resonances. Kaiser and Benner (2009) reported that open ocean LMW DOM exhibited lower abundances of hydrophobic amino acids and total neutral sugars than the HMW counterpart, and this may explain the correlation reported in Table 5.

PC1 has been interpreted as an index of degradation (Dauwe et al., 1999; Amon et al., 2001; Yamashita and Tanoue, 2003; Kaiser and Benner, 2009). But as the PCA derived in this study was correlated with both the long-term degradation signal represented by AOU, and more rapid signals related to picoplankton activity, the PCA results do not favor either hypothesis that attempts to explain variability in %AA-UDOC or amino acid

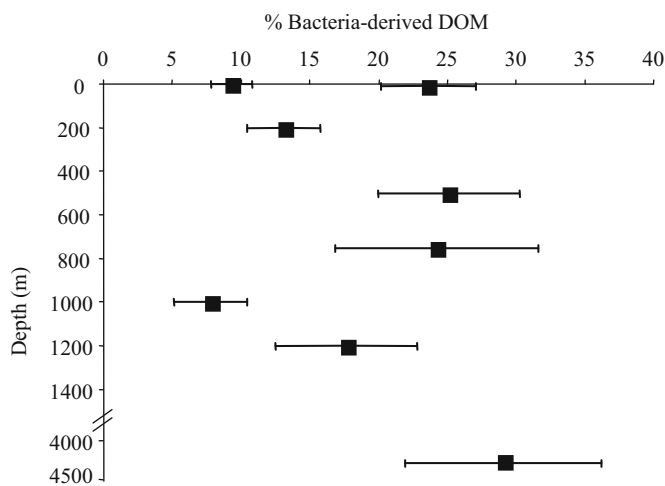


Fig. 9. Average %bacteria-derived DOM, after Kaiser and Benner (2008), see text for discussion. Error bars represent one standard deviation.

distribution noted above (e.g., selective degradation versus alternative metabolism). While D- amino acids in cluster IV are considered more refractory and the observed positive correlation with AOU agrees with this prediction, D-amino acids are also known to be produced and metabolized by marine picoplankton in the deep ocean (Pérez et al., 2003; Teira et al., 2006; Kaiser and Benner, 2008; Varela et al., 2008). The variability captured by PC1 may derive from the relative enhanced contribution of these organisms to production in the deep ocean.

Kaiser and Benner (2008) suggested the use of relative abundances of D- amino acids (D-AA) to TOC as a biomarker for bacteria-derived DOM. We estimated the bacterial contribution to TOC in the EMS using yields determined in this study and end-member estimates of D- AA yields in DOM produced by bacteria in culture (0.29, 0.20, and 0.42 nmol D-AA $\mu\text{mol TOC}^{-1}$ for D-Asp, D-Glu, and D-Ala, respectively; Kaiser and Benner, 2008) using the equation:

$$\% \text{Bacteria-derived DOM} = 100 \times \frac{(\text{D-AA}/\text{TOC})_{\text{sample}}}{(\text{D-AA}/\text{TOC})_{\text{culture}}}$$

Average values ranged from 8 to 29% of TOC for all UDOM samples (including the deep N. Aegean, Fig. 9); these values are similar to those reported throughout the water column and at the BATS and HOT sites (Kaiser and Benner, 2008), but there were large standard deviations in estimates generated by the three D-AA biomarkers (coefficient of variation ranged from 16 to 34%). Bacteria-derived DOM was not correlated with PC1 (and thus not with AOU, picoplankton abundance, or activity). This was unexpected, considering that the variability of the D-AA biomarkers used for this calculation appear to drive PC1, and may be a result of comparing amino acid signatures (described by the PCA) with absolute amino acid concentrations (used for this calculation). The lack of correlation of bacteria-derived DOM with PC1 suggests that there was no significant accumulation of the amino acid component of this flux of DOM. Bacteria-derived DOM in subsurface samples ($n = 6$) was correlated with PC3 however ($r = 0.87$, $p < 0.05$), which explained 9% of amino acid distribution variability and was also correlated with UDOC ($r = 0.82$, $p < 0.05$).

Estimates of bacteria-derived DOM rely on D-AA yields in DOM produced by bacteria cultures; coefficients of variation range from 12 to 43% (Kaiser and Benner 2008) and must thus be interpreted with caution. As discussed above, the amino acid component of UDOC was tightly coupled to picoplankton activity whereas that of bulk DOC was not (Fig. 4); therefore, D-AA may serve as a more

accurate biomarker index of bacteria-derived DOM contribution if calculated normalized to UDOC rather than TOC. Further assessment of this parameter will require a larger collection of subsurface UDOM samples and a more thorough understanding of the production of D-AA by marine picoplankton in culture.

PC2 also described a substantial portion of amino acid mole % variability (31%) but was not correlated with any parameters measured in this study; as such, we are unable to interpret the variability associated with this axis or the fluxes that affect the amino acids in cluster I and III. The primary controls of the distribution of these amino acids appear to differ from clusters II and IV and may result in different residence times of these amino acids in seawater. Martín-Cuadrado et al. (2007) found that genes for the metabolism of glycine, serine, and threonine (from clusters II and IV) were among the most frequent observed in picoplankton collected from the deep Ionian Sea (second only to ABC transporters). Genes for metabolism of cluster I amino acids were also present but $\sim 30\%$ less frequent. Genes for carbohydrate biosynthesis and metabolism genes were almost an order of magnitude less frequent than those for amino acids.

3.6.2. Monosaccharide PCA

PC1 and PC2 accounted for 36% and 25%, respectively, of the variability in monosaccharide distributions. The biplot of PC1 and PC2 loadings of individual monosaccharides were more scattered than those for amino acids (Fig. 8b) and no clusters were identifiable. Galactose and the methyl-sugars (i.e., rhamnose and fucose, also deoxy-sugars) exhibited the greatest positive and negative loadings for PC1, respectively; xylose and mannose had the greatest positive and negative loadings for PC2, respectively. While these monosaccharides exhibited the highest absolute factor loading values for PC1 and PC2, several monosaccharides demonstrated relatively large factor loadings in both dimensions (Fig. 8b) and cannot be ignored when considering the variability captured by PCA.

No site-specific parameters measured in this study were immediately identified as correlated with PC1 scores of UDOM monosaccharide mol % (i.e., $p > 0.05$ for all comparisons), indicating that the primary mechanism that determines monosaccharide distributions is extremely dynamic and seemingly unrelated to other site-specific parameters determined in this study. The carbohydrate component of DOM is considered to be reactive given the large changes in carbohydrate abundance between surface and deep DOM (e.g., Repeta and Aluwihare, 2006). Even though glucose and galactose mol % were significantly correlated with AOU when considered individually (Table 3), and these monosaccharides exhibit opposite loadings for PC1 (Fig. 8b), we do not observe a significant correlation between PC1 and AOU. The highly positive PC1 factor loadings for methyl-sugars (Fig. 8b) reveal that the distributions of these monosaccharides (which were not correlated to AOU; Table 3) are an important source of variability in these UDOM samples. Biogeochemical fluxes related to the turnover of methyl-sugars may thus alter monosaccharide distributions and suppress the remineralization trends that are related to processes driving variability in galactose, glucose, and AOU. The D-AA biomarker index for bacteria-derived DOM (see previous section; Kaiser and Benner, 2008) was significantly correlated with PC1 of monosaccharide distribution ($r = 0.87$, $p < 0.05$). Thus, while the D-AA based estimation of DOM contributed by bacteria did not appear to be associated with amino acid PCA, this contribution may be represented in the monosaccharide component of DOM and may represent the alternative flux associated with mol % of methyl-sugars.

Similarly to PC1 of amino acid distributions, several parameters were correlated with PC2 scores (Table 5). %NS-UDOC and DOC were significantly correlated with PC2 ($r = 0.60$, and 0.77 , respectively; $p < 0.05$). $^1\text{H-NMR}$ resonances were also well correlated with PC2 ($r = -0.85$, -0.83 , and 0.85 for ^1H -aliphatic, alpha-sub, and hetero-sub resonances, respectively, $p < 0.005$; Table 5). DCAA also showed a strong correlation with PC2 ($r = 0.96$, $p < 0.005$). Here we observe another correlation between the two different fractions of UDOM (diafiltered versus non-diafiltered) and this correlation may result from the losses during diafiltration. % DOC retention showed no significant correlations with any PC derived from monosaccharide distribution (Table 5), again suggesting that potential variability introduced as a result of sampling procedures had no effect on variability of monosaccharide distributions. Additional correlations with PC2 include salinity, σ_θ , and AOU; these relationships are driven by surface or low-salinity end-members and may not identify a continuous trend. In summary, correlations reported for PC2 of monosaccharides represent both depth-related and composition-related parameters, and these appear to vary with relative abundances of galactose, xylose, and fucose, and inversely with glucose, mannose, arabinose, and rhamnose.

4. Conclusions

UDOM sampled from a variety of depths in the EMS targeted spatially distinct surface waters as well as subsurface water masses that have been subducted below the euphotic zone for different periods of time, thus exhibiting a range in AOU values. A negative correlation between DOC and AOU observed in this study indicates that remineralization of semi-labile DOC can account for $27 \pm 18\%$ of oxygen consumption in the subsurface EMS (Fig. 3). This is higher than previous reports in the bathypelagic open ocean waters (i.e., $< 10\%$; Hansell, 2002; Aristgui et al. 2002) and consistent with new reports for the Mediterranean Sea (Santinelli et al., 2010). DOC exported from surface waters thus serves as a more important substrate for carbon respiration in the warm ($> 13^\circ\text{C}$), deep waters of the EMS. DOC values were also closely associated with picoplankton abundance and activity (Fig. 4), similar to relationships observed in estuarine systems (e.g., Wetzel 1992, Fernandes et al. 2008) but rare for the open ocean (e.g., Carlson and Ducklow, 1995; Kaartokallio et al., 2007).

While UDOM amino acids are a small component of DOC in the EMS (avg. \pm SD = $0.33 \pm 0.14 \mu\text{mol C L}^{-1}$), we observed strong correlations between the relative amino acid component of UDOM (%AA-UDOC) and AOU and picoplankton activity in water masses of the EMS ($p < 0.002$), but no correlation with DCAA (Figs. 6 and 7). These are strikingly significant correlations between independent measures of the amino acid composition of UDOM and the picoplankton community. The strong correlations observed in Figs. 6 and 7 indicate direct connections between the amino acid component of UDOC and picoplankton carbon pools in seawater, and may thus represent controls on the equilibrium between microbial assemblages and DOM within the microbial loop. In addition, amino acid and monosaccharide distributions, as well as $^1\text{H-NMR}$ spectra were significantly correlated with AOU (Tables 3 and 4). These trends did not extend to the UDOM sample collected in the deep N. Aegean basin, which exhibited low DOC and amino acid abundances, but a $^1\text{H-NMR}$ spectrum and amino acid and monosaccharide mole distribution patterns similar to that found in the surface ocean (Fig. 5, Tables 3 and 4).

PCA revealed that the principal component of variability of amino acid distributions (i.e., PC1, explaining 48% of variability)

was well correlated with %AA-UDOC and picoplankton activity but inversely correlated with AOU. PC1 was also correlated with several other site-specific parameters (Table 5). The PC1 axis captured the mole % variability of two inversely-correlated clusters of amino acids: alanine, serine, tyrosine, and threonine/histidine (cluster II) and D-alanine, D-aspartic acid, D-glutamic acid, and glycine (cluster IV; Fig. 8a), with cluster II amino acids being relatively more enriched in UDOM with high %AA-UDOC and sampled from regions with higher picoplankton activity and lower AOU. We were unable to determine if these signatures were driven by 1) remineralization processes associated with semi-labile DOM that was exported from the surface ocean, which occur over relatively long timescales, or 2) more rapid DOM production and remineralization processes driven by local picoplankton communities that also change with depth (e.g., De Corte et al. 2009). D- amino acid concentrations were used as quantitative biomarkers to estimate the % of TOC contributed by bacteria (according to Kaiser and Benner, 2008). This analysis suggested that bacteria produced 8–29% of DOM in samples collected from the surface to 4350 m in the E. Mediterranean, but this parameter was not correlated with PC1 of amino acid distributions. The flux of DOM produced by bacteria thus does not appear to have accumulated or contributed significantly to the observed variability in amino acid signatures. This observation, together with the significant correlation observed between AOU and PC1, argue for the construction of amino acid distributions by remineralization processes that occur over long timescales. However, the strong correlation between %AA-UDOC and picoplankton activity, which is representative of carbon turnover on a much faster timescale, suggests that more rapid and transient remineralization or alternative production signatures may also be associated with increasing AOU. Together, these observations imply that the principal component of variability in amino acid distributions is not well-defined and will require more extensive study to be categorically assigned as an index of “degradation” or as an alternative biogeochemical flux. This conclusion is consistent with similar analyses in the open ocean (Meador, 2008; Kaiser and Benner, 2009).

Monosaccharide distributions appeared to be more dynamic, as PC1 (explaining 36% of variability) was uncorrelated with most site-specific parameters and it was PC2 (explaining 25% of variability) that showed correlations with %NS-UDOC, DOC, and other site-specific parameters (Table 5). Mole % of galactose and glucose were significantly correlated with AOU, similar to previous reports (McCarthy et al., 1996; Skoog and Benner, 1997; Amon and Benner, 2003; Goldberg et al., 2009), but the AOU signal was not strongly associated with PC1 or PC2. Fluxes associated with AOU thus do not appear to significantly influence monosaccharide distributions. PC1 was correlated with estimates of bacteria-derived DOM however, indicating that the flux of carbohydrates produced by bacteria may accumulate more significantly than that of proteins.

These collaborative analyses have begun to elucidate key relationships that connect DOM chemical characterization to heterotrophic metabolism and marine biogeochemical cycles. The chemical characterization of DOM in the EMS provided by this study represents the first such data for this region, and the enhanced respiration of DOC in the relatively warm “twilight” zone of the EMS was advantageous for establishing explicit correlations in DOM cycling, thus advocating for additional investigations of DOM and microbial composition dynamics in this unique region. Advancements in interpreting UDOM composition signals will rely, in part, on detailed studies targeting metabolism of the key amino acids and monosaccharides identified by this and other studies, and also on information provided by the intact macromolecules from which these signals were derived.

Acknowledgments

TBM and AG acknowledge funding from the Hellenic GSRT/European Union (non-EU Grant No180) and SESAME Project (European Commission's Sixth Framework Program, EC Contract No GOCE-036949). TY was supported by the Japanese Society for the Promotion of Science (JSPS) Postdoctoral Fellowship for research abroad and DDC received a fellowship of the University of Groningen. Microbial laboratory work and molecular analyses were supported by a grant of the Earth and Life Science Division of the Dutch Science Foundation (ARCHIMEDES project, 835.20.023) to G.J.H. DJR and TBM were supported by grants from the Gordon and Betty Moore Foundation and from the C-MORE organization of NSF. We gratefully acknowledge D. Georgopoulos, V. Lykousis and D. Ballas (HCMR) for kindly offering ship time during the POSEIDON and KM3Net cruises, and the captain, officers and the crew of R/V Aegaeo for their generous assistance at sea. A. Antoniadis and G. Katsouras are acknowledged for their heroic assistance during the collection of UDOM samples. We acknowledge the organizers of the 2008 IMBER IMBIZO, anonymous reviewers, and D. Hansell for their efforts and assistance in the preparation of this manuscript. This work was performed within the 'Network of Excellence' EuroOceans supported by the 6th Framework Program of the European Union.

References

- Aluwihare, L.I., Repeta, D.J., Chen, R.F., 1997. A major biopolymeric component to dissolved organic carbon in surface seawater. *Nature* 387, 166–169.
- Aluwihare, L.I., Repeta, D.J., Chen, R.F., 2002. Chemical composition and cycling of dissolved organic matter in the Mid-Atlantic Bight. *Deep-Sea Research II* 49, 4421–4437.
- Aluwihare, L.I., Meador, T.B., 2008. Chemical composition of marine dissolved organic nitrogen. In: Capone, D.G., Bronk, D.A., Mulholland, M.R., Carpenter, E.J. (Eds.), *Nitrogen in the Marine Environment* 2nd edition Elsevier, Netherlands, pp. 95–133.
- Amon, R.M.W., Fitznar, H-P, Benner, R., 2001. Linkages among the bioreactivity, chemical composition, and diagenetic state of marine dissolved organic matter. *Limnology and Oceanography* 46 (2), 287–297.
- Amon, R.M.W., Benner, R., 2003. Combined neutral sugar as indicators of the diagenetic state of dissolved organic matter in the Arctic Ocean. *Deep-Sea Research I* 50, 151–169.
- Anderson, L.A., Sarmiento, J.L., 1994. Redfield ratios of remineralization determined by nutrient data-analysis. *Global Biogeochemical Cycles* 8 (1), 65–80.
- Aristegui, J., Duarte, C.M., Agustí, S., Doval, M., Álvarez-Salgado, X.A., Hansell, D.A., 2002. Dissolved organic carbon support of respiration in the dark ocean. *Science* 298, 1967.
- Azam, F., Fenchel, T., Field, J.G., Gray, J.S., Meyer-Reil, L.A., Thingstad, F., 1983. The ecological role of water-column microbes in the sea. *Marine Ecology Progress Series* 10, 257–263.
- Benner, R., Pakulski, J.D., McCarthy, M., Hedges, J.L., Hatcher, P.G., 1992. Bulk chemical characteristics of dissolved organic matter in the ocean. *Science* 255, 1561–1564.
- Benner, R., Biddanda, B., Black, B., McCarthy, M., 1997. Abundance, size distribution, and stable carbon and nitrogen isotopic compositions of marine organic matter isolated by tangential-flow ultrafiltration. *Marine Chemistry* 57, 243–263.
- Béthoux, J.P., Morin, P., Ruiz-Pino, D., 2002. Temporal trends in nutrient ratios: chemical evidence of Mediterranean ecosystem changes driven by human activity. *Deep-Sea Research II* 49, 2007–2016.
- Brix, H., Gruber, N., Karl, D.M., Bates, N.R., 2006. On the relationships between primary, net community, and export production in subtropical gyres. *Deep-Sea Research II* 53, 698–717.
- Carlson, C.A., 2002. Production and removal processes. In: Matter, D.A., Hansell, D.A., Carlson, C.A. (Eds.), *Biogeochemistry of Marine Dissolved Organic*. Academic Press, San Diego, pp. 91–139.
- Carlson, C.A., Ducklow, H.W., Michaels, A.F., 1994. Annual flux of dissolved organic carbon from the euphotic zone in the Northwestern Sargasso Sea. *Nature* 371, 405–408.
- Carlson, C.A., Ducklow, H.W., 1995. Dissolved organic carbon in the upper ocean of the central Equatorial Pacific, 1992: Daily and fine-scale vertical variations. *Deep-Sea Research II* 42, 639–656.
- Carlson, C.A., Hansell, D.A., Nelson, N.B., Siegel, D.A., Smethie Jr., W.M., Khattiwala, S., Meyers, M.M., Wallner, E., 2010. Dissolved organic carbon export and subsequent remineralization in the mesopelagic and bathypelagic realms of the North Atlantic basin. *Deep Sea Research II* 57 (16), 1433–1445.
- Carpenter, J.H., 1965a. The accuracy of the Winkler method for the dissolved oxygen analysis. *Limnology and Oceanography* 10, 135–140.
- Carpenter, J.H., 1965b. The Chesapeake Bay Institute technique for dissolved oxygen method. *Limnology and Oceanography* 10, 141–143.
- Cherrier, J., Bauer, J.E., Druffel, E.R.M., 1996. Utilization and turnover of labile dissolved organic matter by bacterial heterotrophs in eastern North Pacific surface waters. *Marine Ecology Progress Series* 139, 267–279.
- Copin-Montegut, G., Avril, B., 1993. Vertical distribution and temporal variation of dissolved organic carbon in the North-Western Mediterranean Sea. *Deep-Sea Research* 40, 1963–1972.
- Dauwe, B., Middelburg, J.J., Herman, P.M.J., Heip, C.H.R., 1999. Linking diagenetic alteration of amino acids and bulk organic matter reactivity. *Limnology and Oceanography* 44 (7), 1809–1814.
- De Corte, D., Yokokawa, T., Varela, M.M., Agogué, H., Herndl, G.J., 2009. Spatial distribution of *Bacteria* and *Archaea* and *amoA* gene copy numbers throughout the water column of the Eastern Mediterranean Sea. *The ISME Journal* 3, 147–158.
- Doval, M.D., Hansell, D.A., 2000. Organic carbon and apparent oxygen utilization in the western South Pacific and the central Indian Oceans. *Marine Chemistry* 68, 249–264.
- Druffel, E.R.M., Bauer, J.E., Williams, P.M., Griffin, S., Wolgast, D., 1996. Seasonal variability of particulate organic radiocarbon in the northeast Pacific Ocean. *Journal of Geophysical Research* 101 (C9), 20543–20552.
- Fernandes, V., Ramaiah, N., Paul, J.T., Sardesai, S., Babu, R.J., Gaums, M., 2008. Strong variability in bacterioplankton abundance and production in central and western Bay of Bengal. *Marine Biology* 153, 975–985.
- Fitznar, H.-P., Lobbes, J.M., Kattner, G., 1999. Determination of enantiomeric amino acids with high-performance liquid chromatography and pre-column derivatisation with o-phthalaldehyde and N-isobutyrylcysteine in seawater and fossil samples (mollusks). *Journal of Chromatography* 832 (1–2), 123–132.
- Fukuda, R., Ogawa, H., Nagata, T., Koike, I., 1998. Direct determination of carbon and nitrogen contents of natural bacterial assemblages in marine environments. *Applied and Environmental Microbiology* 64 (9), 3352–3358.
- Gertman, I., Pinardi, N., Popov, Y., Hecht, A., 2006. Aegean Sea water masses during the early stages of eastern Mediterranean climatic transient. *Journal of Physical Oceanography* 36, 1841–1859.
- Goldberg, S.J., Carlson, C.A., Hansell, D.A., Nelson, N.B., Siegel, D.A., 2009. Temporal dynamics of dissolved combined neutral sugars and the quality of dissolved organic matter in the Northwestern Sargasso Sea. *Deep-Sea Research I* 56, 672–685.
- Guo, L., Santschi, P.H., Cifuentes, L.A., Trumbore, S.E., Southon, J., 1996. Cycling of high-molecular-weight dissolved organic matter in the middle Atlantic bight as revealed by carbon isotopic (¹³C and ¹⁴C) signatures. *Limnology and Oceanography* 41 (6), 1242–1252.
- Hansell, D.A., 2002. DOC in the global ocean carbon cycle. In: Matter, D.A., Hansell, D.A., Carlson, C.A. (Eds.), *Biogeochemistry of Marine Dissolved Organic*. Academic Press, San Diego, pp. 685–715.
- Hansell, D.A., Carlson, C.A., 2001. Biogeochemistry of total organic carbon and nitrogen in the Sargasso Sea: control by convective overturn. *Deep Sea Research II* 48, 1649–1667.
- Hansell, D.A., Carlson, C.A., 1998a. Deep ocean gradients in dissolved organic carbon concentrations. *Nature* 395, 263–266.
- Hansell, D.A., Carlson, C.A., 1998b. Net community production of dissolved organic carbon. *Global Biogeochemical Cycles* 12, 443–453.
- Hansell, D.A., 1993. Results and observations from the measurement of DOC and DON in seawater using a high-temperature catalytic oxidation technique. *Marine Chemistry* 41, 195–202.
- Hedges, J.L., 1992. Global biogeochemical cycles: progress and problems. *Marine Chemistry* 39, 67–93.
- Hoehler, T.M., 2004. Biological energy requirements as quantitative boundary conditions for life in the subsurface. *Geobiology* 2, 205–215.
- Hubberten, U., Lara, R.J., Kattner, G., 1994. Amino acid composition of seawater and dissolved humic substances in the Greenland Sea. *Marine Chemistry* 45, 121–128.
- Ignatiades, L., 1998. The productive and optical status of the oligotrophic waters of the Southern Aegean Sea (Cretan Sea), Eastern Mediterranean. *Journal of Plankton Research* 20 (5), 985–995.
- Kaartokallio, H., Kuosa, H., Thomas, D.N., Granskog, M.A., Kivi, K., 2007. Biomass, composition and activity of organism assemblages along a salinity gradient in sea ice subjected to river discharge in the Baltic Sea. *Polar Biology* 30, 183–197.
- Kaiser, K., Benner, R., 2005. Hydrolysis-induced racemization of amino acids. *Limnology and Oceanography Methods*, 3, 318–325.
- Kaiser, K., Benner, R., 2008. Major bacterial contribution to the ocean reservoir of detrital organic carbon and nitrogen. *Limnology and Oceanography* 53 (1), 99–112.
- Kaiser, K., Benner, R., 2009. Biochemical composition and size distribution of organic matter at the Pacific and Atlantic time-series stations. *Marine Chemistry* 113, 63–77.
- Karageorgis, A.P., Gardner, W.D., Gergopoulos, D., Mishonov, A.V., Krasakopoulou, E., Anagnostou, C., 2008. Particle dynamics in the Eastern Mediterranean Sea: a synthesis based on light transmission, PMC, and POC archives (1991–2001). *Deep-Sea Research I* 55, 177–202.
- Karner, M., Herndl, G.J., 1992. Extracellular enzymatic activity and secondary production in free-living and marine-snow-associated bacteria. *Marine Biology* 113, 341–347.

- Keil, R.G., Kirchman, D.L., 1994. Abiotic transformation of labile protein to refractory protein in sea water. *Marine Chemistry* 45, 187–196.
- Kirchman, D., 2001. Measuring bacterial biomass production and growth rates from leucine incorporation in natural aquatic environments. In: Paul, J.H. (Ed.), *Methods in Microbiology* (Vol 30): Marine Microbiology. Academic Press.
- Klein, B., Roether, W., Kress, N., Manca, B.B., d'Alcala, M.R., Souvermezoglou, E., Theocharis, A., Civitarese, G., Luchetta, A., 2003. Accelerated oxygen consumption in eastern Mediterranean deep waters following recent changes in thermohaline circulation. *J. Geophysical Research – Oceans*, 108, doi:10.1029/2002JC001454.
- Krasakopoulou, E., Souvermezoglou, E., Pavlidou, A., Kontoyiannis, H., 1999. Oxygen and Nutrient Fluxes through the Straits of the Cretan Arc (March 1994 – January 1995). *Progress in Oceanography* 44, 601–624.
- Krom, M.D., Groom, S., Zohary, T., 2003. The Eastern Mediterranean. In: Black, K.D., Shimmield, G.B. (Eds.), *The Biogeochemistry of Marine Systems*. Blackwell Publishing, Oxford, pp. 91–122.
- Krom, M.D., Brenner, S., Kress, N., Neori, A., Gordon, L.L., 1992. Nutrient dynamics and new production in a warm-core eddy from the E Mediterranean. *Deep-Sea Research* 39, 467–480.
- Lasaratos, A., 1993. Estimation of deep and intermediate water mass formation rates in the Mediterranean Sea. *Deep-Sea Research II* 40, 1327–1332.
- Martín-Cuadrado, A.-B., López-García, P., Alba, J.-C., Moreira, D., Monticelli, L., Strittmatter, A., Gottschalk, G., Rodríguez-Valera, F., 2007. Metagenomics of the deep Mediterranean, a warm bathypelagic habitat. *PLoS One* 2, e914.
- McCarthy, M., Hedges, J., Benner, R., 1996. Major biochemical composition of dissolved high molecular weight organic matter in seawater. *Marine Chemistry* 55, 281–297.
- McCarthy, M., Hedges, J., Benner, R., 1998. Major bacterial contribution to marine dissolved organic nitrogen. *Science* 281, 231–234.
- Meador, T.B., Aluwihare, L.L., Mahaffey, C., 2007. Isotopic heterogeneity and cycling of organic nitrogen in the oligotrophic ocean. *Limnology and Oceanography* 52 (3), 934–947.
- Meador, T.B. 2008. A spatial deconvolution of molecular signals in oceanic dissolved organic matter. UC San Diego: Scripps Institution of Oceanography. Retrieved from: < <http://escholarship.org/uc/item/55d4w9xc> >.
- Murphy, J., Riley, J.P., 1962. A modified solution method for determination of phosphate in natural waters. *Analytica Chimica Acta* 27, 31–36.
- Myers, P.G., Haines, K., 2000. Seasonal and interannual variability in a model of the Mediterranean under derived flux forcing. *Journal of Physical Oceanography* 30 (5), 1069–1082.
- Mykkestad, S.M., Skanøy, E., Hestmann, S., 1997. A sensitive and rapid method for analysis of dissolved mono- and polysaccharides in seawater. *Marine Chemistry* 56, 279–286.
- Nagata, T., Fukuda, H., Fukuda, R., Koike, I., 2000. Bacterioplankton distribution and production in deep Pacific waters: Large-scale geographic variations and possible coupling with sinking particle fluxes. *Limnology and Oceanography* 45, 426–435.
- Nagata, T., Tamburini, C., Aristegui, J., Baltar, F., Bochdansky, A., Fonda-Unami, S., Fukuda, H., Gogou, A., Hansell, D.A., Hansman, R.L., Herndl, G., Panagiotopoulos, C., Reintharler, T., Sohrin, R., Verdugo, P., Yamada, N., Yamashita, Y., Yokokawa, T., Bartlett, D.H., 2010. Emerging concepts on microbial processes in the bathypelagic ocean – ecology, biogeochemistry and genomics. *Deep Sea Research II* 57 (16), 1519–1536.
- Panagiotopoulos, C., Sempéré, R., 2005. Analytical methods for the determination of sugars in marine samples: a historical perspective and future directions. *Limnology and Oceanography*: Methods 3, 419–454.
- Pérez, M.T., Paus, C., Herndl, G.J., 2003. Major shift in bacterioplankton utilization of enantiomeric amino acids between surface waters and the ocean's interior. *Limnology and Oceanography* 48, 755–763.
- Psarra, S., Tselepidis, A., Ignatiades, L., 2000. Primary productivity in the oligotrophic Cretan Sea (NE Mediterranean): seasonal and interannual variability. *Progress in Oceanography* 46, 187–204.
- Repeta, D.J., Aluwihare, L.L., 2006. Radiocarbon analysis of neutral sugars in high-molecular-weight dissolved organic carbon: implications for organic carbon cycling. *Limnology and Oceanography* 51 (2), 1045–1053.
- Roether, W., Klein, B., Manca, B.B., Theocharis, A., Kioroglou, S., 2007. Transient Eastern Mediterranean deep waters in response to the massive dense-water output of the Aegean Sea in the 1990 s. *Progress in Oceanography* 74, 540–571.
- Roether, W., Well, R., 2001. Oxygen consumption in the Eastern Mediterranean. *Deep-Sea Research I* 48, 1535–1551.
- Santinelli, C., Manca, B.B., Gasparini, G.P., Nannicini, L., Serriti, A., 2006. Vertical distribution of dissolved organic carbon (DOC) in the Mediterranean Sea. *Climate Research* 31, 205–216.
- Santinelli, C., Nannicini, L., Serriti, A., 2010. DOC dynamics in meso and bathypelagic layers of the Mediterranean Sea. *Deep Sea Research II* 57 (16), 1446–1459.
- Sempéré, R., Charrière, B., Van Wambeke, F., Cauwet, G., 2000. Carbon inputs of the Rhône River to the Mediterranean Sea: biogeochemical implications. *Global Biogeochemical Cycles* 14 (2), 669–681.
- Sempéré, R., Panagiotopoulos, C., Lafont, R., Marroni, B., Van Wambeke, F., 2002. Total organic carbon dynamics in the Aegean Sea. *Journal of Marine Systems* 33–34, 355–364.
- Serriti, A., Manca, B.B., Santinelli, C., Murru, E., Boldrin, A., Nannicini, L., 2003. Relationships between dissolved organic carbon (DOC) and water mass structures in the Ionian Sea (winter 1999). *Journal of Geophysical Research*, 108, doi:10.1029/2002JC001345.
- Skoog, A., Benner, R., 1997. Aldoses in various size fractions of marine organic matter: implications for carbon cycling. *Limnology and Oceanography* 42 (8), 1803–1813.
- Smith, D., Simon, M., Alldredge, A.L., Azam, F., 1992. Intense hydrolytic enzyme activity on marine aggregates and implications for rapid particle dissolution. *Nature* 359, 139–142.
- Spyres, G., Nimmo, M., Worsfold, P.J., Achterberg, E.P., Miller, A.E.G., 2000. Determination of dissolved organic carbon in seawater using high temperature catalytic oxidation techniques. *Trends in Analytical Chemistry* 19 (8), 498–506.
- Stavrakakis, S., Krasakopoulou, E., Kabouri, G., 2006. Particulate organic carbon fluxes and balance estimation in S. Aegean (SE Mediterranean Sea). *Proceedings of 8th Panhellenic Symposium of Oceanography and Fisheries, Thessaloniki, 4–8 June 2006*, p. 159.
- Strickland, J.D.H., Parsons, T.R., 1972. *A practical handbook of sea water analysis*. Fisheries Research Board of Canada 167, 310.
- Teira, E., v. Aken, H., Veth, C., Herndl, G.J., 2006. Archaeal uptake of enantiomeric amino acids in the meso- and bathypelagic waters of the North Atlantic. *Limnology and Oceanography* 51, 60–69.
- Theocharis, A., Balopoulos, E., Kioroglou, S., Kontoyiannis, H., Iona, A., 1999. A synthesis of the circulation and hydrography of the South Aegean Sea and the Straits of the Cretan Arc (March 1994–January 1995). *Progress in Oceanography* 44, 469–509.
- Toggweiler, J.R., 1989. Is the downward dissolved organic matter (DOM) flux important in carbon transport? In 'Productivity in the Ocean. In: Berger, W.H., Smetacek, V.S., Wafer, G. (Eds.), Present and Past'. Wiley, New York, pp. 65–83.
- Tzipperman, E., Speer, K.G., 1994. A study of water mass transformation in the Mediterranean Sea: analysis of climatological data and a simple 3-box model. *Dynamics of Atmospheres and Oceans* 21, 53–82.
- UNESCO, 1986. *Progress on Oceanographic Tables and Standards 1983–1986. Work and recommendations of the UNESCO/SCOR/ICES/IAPSO Joint Panel. UNESCO Technical Papers in Marine Science*, 50.
- Varela, M.M., van Aken, H.M., Sintes, E., Herndl, G.H., 2008. Latitudinal trends of Crenarchaeota and Bacteria in the meso- and bathypelagic water masses of the Eastern North Atlantic. *Environmental Microbiology* 10 (1), 110–124.
- Wetzel, R.G., 1992. Gradient-dominated ecosystems: sources and regulatory functions of dissolved organic matter in freshwater ecosystems. *Hydrobiologia* 229, 181–198.
- Williams, P.M., Druffel, E.R.M., 1988. Dissolved organic matter in the ocean: comments on a controversy. *Oceanography* 1, 14–17.
- Yamashita, Y., Tanoue, E., 2003. Distribution and alteration of amino acids in bulk DOM along a transect from bay to oceanic waters. *Marine Chemistry* 82 (3–4), 145–160.
- Zervakis, V., Drakopoulos, P.G., Georgopoulos, D., 2000. The role of the North Aegean in triggering the recent Eastern Mediterranean climatic changes. *Journal of Geophysical Research* 105 (C11), 103–126.
- Zervakis, V., Georgopoulos, D., 2002. Hydrology and Circulation in the North Aegean (eastern Mediterranean) throughout 1997–1998. *Mediterranean Marine Science* 3/1, 5–19.
- Zervakis, V., Krasakopoulou, E., Georgopoulos, D., Souvermezoglou, E., 2003. Vertical diffusion and oxygen consumption during stagnation periods in the deep North Aegean. *Deep-Sea Research I* 50, 53–71.
- Zervakis, V., Georgopoulos, D., Karageorgis, A.F., Theocharis, A., 2004. On the response of the Aegean Sea to climatic variability: a review. *International Journal of Climatology*, 24.